Fabrication, Structural Characterization, Electric and Dielectric Parameters of the Laboratory Synthesized Nano-Crystalline Erbium Oxide (Er_2O_3)

Fahad Azad
2011-NUST-MPhil PhD-Phy-04

Supervised by

Meritorious Professor

Dr. Asghari Maqsood, (SI)

Fellow Pakistan Academy of Sciences (PAS),
Center for Emerging Sciences, Engineering and Technology (CESET)
Islamabad, Pakistan

This Dissertation is dedicated to my Mother and Father

I would like to spend my lifetime loving you,
If that is all in life I will ever do...

Acknowledgements

I would like to sincerely thank Almighty Allah for His blessings...

During this work, there were so many people whose support, direction, advice and contribution have proved invaluable. In particular, I owe my deepest gratitude to my mentor distinguished National Prof. Dr. Asghari Maqsood for all her help, advice and patience over the last year. Her enthusiasm and unlimited zeal has been the major driving force for this research work. I would also like to acknowledge my guidance committee members Dr. Fahim Ameen, Dr. Iftikhar H. Gul and Dr. Aurangzeb, they all helped me to the extent they could do.

I am indebted to the Principal of my School "Prof. Dr. Azad Akhter Siddiqui" who allowed me to pursue my research in experimental Physics, it wouldn't have been possible without his backing and struggle. I cannot find words to express my gratitude to the head of Physics department "Dr. Ayesha Khalique", she is very well behaved and a pulchritudinous lady. It is my great pleasure to acknowledge the support and help provided by Dr. Rizwan Khalid. I consider it an honor to work under the kind supervision of this great physicist, as a lab demonstrator in Physics Labs. I am feeling wordless to thank him for all his assistance, he has ever done. I am thanking "Dr. Ruby Gul" most warmly for her generous contribution in making me understand some significant concepts of the present work.

A very special thank to my friends Muhammad Javad, Waqar Azeem and Aqib Afaq who were always with me to share every thick and thin during this time. I would also like to acknowledge the beautiful moments, spent with Usama Zaheer and Saqib Hussain.

I am thankful to School of Chemical and Material Engineering for allowing me to use their labs. Furthermore, I am grateful to all the technical staff for their support. PSF project 147 is acknowledged for the grant of funds to purchase LCR meter, used in this research.

Fahad Azad

Contents

List of Figures

Abstract

Nano crystalline erbium oxide (Er_2O_3) was synthesized from its nitrate precursor using sol-gel method, in the laboratory. X-ray diffraction (XRD) was used to investigate the effect of different annealing temperatures on its crystal structure and the data have been used to calculate the specific surface area (s), average crystallite size (t) and xrd density of the samples. Specific surface area (s) was also measured using Brunauer, Emmett & Teller theory , and results were found in agreement with the specific surface area calculated using (XRD) with a maximum error of approximately 7%. To study the morphology of samples the scanning electron microscope (SEM) was used; it disclosed a spherical morphology for particles while a flaky morphology for the films. For elemental analysis of erbium oxide energy dispersive spectroscopy (EDS) of the synthesized samples was also carried out. An increase in surface activity was noticed in sample annealed at lower temperature because of the small crystallite size and larger specific surface area, in the fourier transform infrared (FTIR) spectroscopy of the samples. Furthermore, the finger print region of the spectrum showed the characteristic peaks for Er-O and Er-O-Er stretching. The dielectric properties in the range (100 Hz - 5 MHz) of frequency showed the frequency dependance of the dielectric constant and the trend of the dielectric properties was in agreement with that reported in literature but with enhanced dielectric constant. The electric properties of the erbium oxide suggested it a mixed conductor with some contribution from ionic conductivity while a major contribution from the p-type electronic conductivity. From the onset of ionic conductivity, the activation energy of erbium oxide were found to increase as the temperature increased beyond a break temperature T_B. Hall effect measurements revealed that the synthesized erbium oxide pellets and films behave like a p-type semiconductors. The measurement of the important parameters of Hall characterization in the temperature range (300 K -350 K) suggested the material to have useful applications in the Hall effect sensors (HES); because of its thermal stability at extreme temperatures and high sensitivity at lower temperatures.

Chapter 1

Introduction

1.1 Nanoscience

Nanoscience can be defined by a common working definition as "The study of phenomena and manipulation of materials at atomic, molecular and macromolecular scales, where properties differ more significantly from those at larger scale" [1]. The bulk materials obey the principle of classical mechanics but when it comes to nanomaterials the principles of classical mechanics fail to explain the phenomena rather quantum mechanics principles have found to be very useful in explaining the world of nano. The same material (e.g, gold) at the nano scale can have properties (e,g, optical, mechanical, electrical etc.) which are very different from (even opposite to!) the properties of materials at the macroscale (bulk) [2].

1.2 Historical Overview of Nano-Science and Nano-Technology

In 1959, Richard Feynman gave a lecture "There is plenty of room at the bottom" which is often mentioned when people talk about the nanoscience and nanotechnology. He predicted that if we succeeded in arranging molecules or atoms in the way we want, substances with extremely great range of properties can be made. However, research in nano science took off a few decades back.
The 20^{th} century has been designated as the century of physics because of the revolutionary work done in Physics and its enormous impact. A remarkable foundation has established in explaining nature at the nano level on the one hand and the universe's evolution on the other hand. Quantum mechanics helped in understanding the nature of molecules, atoms and solids, while the solid state physics assisted in the development of semiconductor science and engineering.
Our exploitation and understanding of the material world around us is going in two different directions, bottom-up and the top-down. In the bottom up approach building blocks are atoms and molecules. The nature of atoms and simple molecules has been explained however we are still work-

ing to understand the behavior of the complex molecules, polymers, clusters at the nanoscale. The interest in reducing the size of the devices has increased as a result of which building blocks of the electronic industry (resistors, transistors and capacitors etc) have been made on the micron level. Both the bottom up and top down approaches have independently developed in the past largely but today both are meeting at the nano scale. People at top down territory need to consider nature's behavior at the atomic level while the stream in the bottom up approach are going to fabricate novel remarkable devices with atoms and molecules as the building units. It is important to note that these atomic level devices are not only just part of scientific literature rather it has an indispensable impact on our computers, cars, mobile phones and even on the appliances for daily use. Just take the metal oxide semiconductor field effect transistor (MOSFET) as an example, the block diagram of MOSFET is shown in figure 1.1. MOSFET's in these days have a length of channel approximately

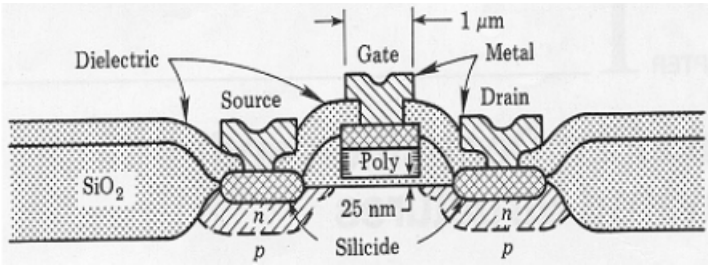

Figure 1.1: Block Diagram of MOSFET

0.1 μm and a thickness of gate oxide about 2-3 nm, which is about 10 times smaller as compared to that shown in the fig 1.1. Any further decrease in the gate oxide thickness will result an increase of leakage current and electrical breakdown during device operation easily. The channel length cannot be further shrank because it would result a tunneling current from the source to the drain. Now engineers in the microelectronic industry are very interested in the analysis of the devices at nanoscale. The scaling down of the devices reducing cost and energy consumption of operation.

Nanoscience and Nanotechnology are both in the development stages. Although a lot of theoretical and experimental work has been done but still understanding of the fundamentals is still to be searched. The domain of nanoscience and nanotechnology is not well defined because both are still expanding. Nanoscience and nanotechnology are considered as the pillars of the economy based on knowledge and these fields are drawing interest of both the communities in and out of academics.

1.3 Nanomaterials

A material with at least one physical dimension in the nanoscale is termed as nanomaterial. The nanoscale range is defined as 0-100 nm conventionally. Nanomaterials have raised their interest amongst engineers and scientists, from nearly all the industries, in developing new technology and in the improvement of the existing. Here a question arises, what makes the nanomaterials so important and special? There are several reasons for why they are so promising. Firstly, their size make them behave so and quantum size effect is the reason for making their properties completely divergent from their bulk counterparts. For example the silver in the bulk form is harmless while its nanoparticles help to kill viruses [3]. Secondly, the fabrication method is the another thing that can cause nanomaterials to behave differently. Finally, as the size decrease the ratio between surface area to the volume increases as compared to the bulk material and becomes the reason for nanoparticles strange behavior in the processes which takes place at surface.

1.3.1 Classification of Nano materials

The nano materials can be classified in four different groups based on the number of dimensions that are not confined in the nanoscale range.

1.Zero Dimensional 2.One Dimensional 3.Two Dimensional 4.Three Dimensional

Zero dimensional nano-structures

Those material in which all three dimensions lies in nanoscale range ($\leq$100 nm) are called as zero dimensional nanomaterials. They include nano particles, quantum dots, nanoshells, nanorings and micro capsules.

One dimensional nano-structures

Those materials in which two dimensions are in nanoscale range or the electrons are free to move in one dimension are termed as the one dimensional nanomaterials. They include Nanotubes, Nanofibres and nanowires.

Two dimensional nano-structures

These are the materials in which one dimension lies in the nanoscale range. In these materials electrons are confined in the one dimension and they are free to move in the other two. The two dimensional nano structure includes nanofilms, nano coatings and layers.

Three dimensional nano-structures

These are the bulk nano materials having no dimension in the nano range ($\leq$100nm) rather having above described nano structure embedded in. These materials do not lie in nanorange but still they have very unique and interesting properties because of the nano structures present inside it.

1.4 Properties of Nanomaterials

Nanomaterials lie in between atoms and bulk with respect to their structure. The most of the materials with the physical dimensions in the range of microns have similar properties as their bulk but the materials with dimension in nanometers have strange and completely different properties from those of atoms or bulk. This change in properties is mainly due to (i) quantum confinement, (ii) greater surface energy, (iii) large fraction of surface atoms, and (iv) reduced imperfections, which were not in the bulk material.

The quantum confinement effect induce discrete energy levels for electrons and the band structure changes as compared to that of bulk. So, the materials are going to have modified electronic and optical properties. For example quantum dots and quantum wires have found to be very useful in devising laser and light emitting diodes. As the size of nanomaterials is very small so they have an extremely large surface to volume ratio as a result of which they have larger number of interfacial atoms. So this thing enhance the materials surface properties as compared to the bulk. For example, the chemical sensors made up of the nanoparticles has enhanced sensitivity and selectivity, similarly metallic nanoparticles have been proved active catalysts. The increased perfection of the materials makes them to exhibit more chemical stability and enhanced mechanical properties. The noticeably improved mechanical properties of carbon nanotubes are well known.

1.4.1 Optical Properties

The optical properties of nanomaterials are the most fascinating and useful. Due to their unique and interesting optical properties nanomaterials have been very important in imaging, solar cells [4], optical sensors [5], phosphor [6], laser [7], photocatalysis [8], sensors and biomedicine [9, 10]. The optical properties depends on shape, size, surface, doping and the environment (other nano structures) surrounding it [11]. Shape has a dramatic effect on the optical properties in the nanostructures of the metals.

The figure is showing the difference between the optical properties of the metals and semicon-

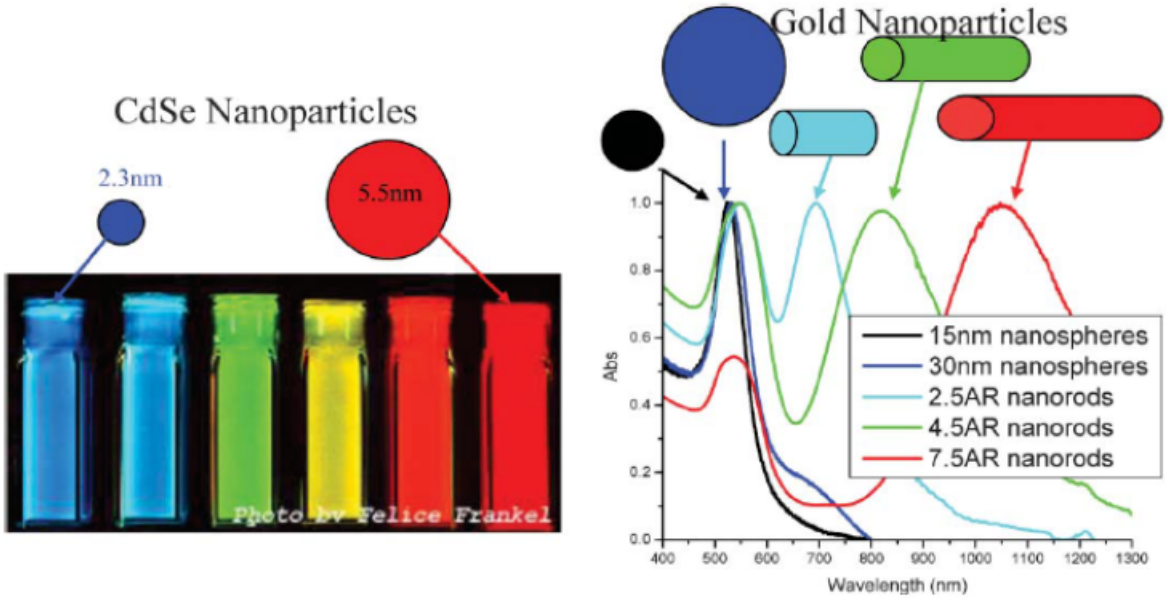

Figure 1.2: Fluorescence in CdSe quantum dots and the absorption spectra of gold nano structures of various shape and size [12].

ductors. Only the change in size cause the semiconductor nano particles to change their optical properties while nanoparticles of metals shows a slight difference in their properties with the change in the size. Nonetheless when anisotropy is added to the material, the optical properties show a vivid change

1.4.2 Electrical properties

Electrical properties of nano materials describe the electrical conductivity or electrical resistivity. As the size of nano materials is very small so the number of electron wave modes contributing in the conduction process gets increasingly smaller by quantized steps. For example in carbon nanotubes only one electron wave mode has been observed which was responsible for conduction of the material [13].

There are so many methods for studying electrical properties. One interesting method to find electrical resistance of material by measuring the current passing through the nanostructure (let's say nanowire) by applying the constant voltage. From the resistance and using the dimensions of the sample materials resistivity can easily be calculated. It has also been found that increase in the size causes the electrical resistance to decrease because of the more electron wave modes contributing in the conduction process.

1.4.3 Magnetic Properties

Gold and Platinum are non magnetic in the bulk form while their nanostructures are magnetic. The atoms that lie on the surface are not only different as compared to bulk but they can be modified by capping the surface atoms with appropriate molecules. The phenomena improves the physical properties of the material.

Actually the materials which are non ferromagnetic can be hopped to behave as ferromagnetic in the

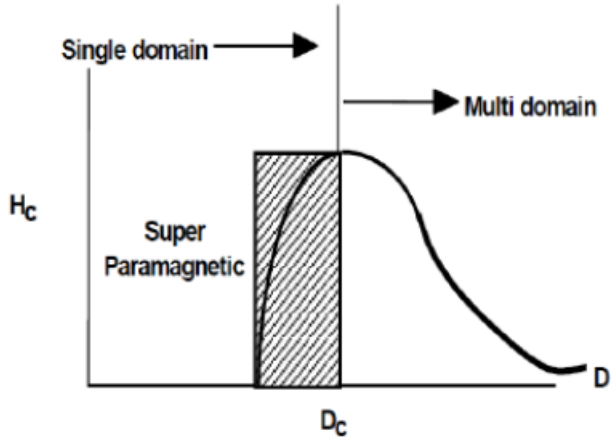

Figure 1.3: Magnetism in nano materials [14]

nano scale. It is very strange to know that gold which is diamagnetic in the bulk shows a magnetic behavior in the nano regime [15] while platinum becomes ferromagnetic because of the structural changes on the nano scale [16]. We can transform gold nanoparticles to behave as ferromagnetic material by capping its nanoparticles with appropriate molecules. Actually the surface charge which is localized at the surface of the particle rises the ferromagnetic behavior. Core and the surface of gold nanoparticles with 2 nm diameter show a paramagnetic and ferromagnetic behavior respectively. Furthermore the permanent magnetism has been noticed at room temperatures by capping the nanoparticles e.g, thiol-capped gold nanoparticles show a permanent magnetic behavior at room temperature.

1.5 Applications of Nanomaterials

Nano materials have been very important in every field of life. They have many applications in the modern technology, fuel cells [17], agriculture [18], medicine [19], food industry [20], and electronics [21]. Few of the applications are discussed here

1.5.1 Fuel cells

Fuel cell is the device that converts chemical energy from fuel (anode side) and oxidant (cathode side) in to electricity. Electrodes are the heart of the fuel cells. The optimization of the fuel cells can be done in two ways:

- by changing the structure of the fuel cell,
- by using some active catalysts.

Surface area of electrodes must be good enough so that it can provide a maximum contact area for catalyst electrolyte and reactant gas. So that it can facilitate gas transport and good conductance. This type of the structure will also decrease the losses.

Microbial Fuel Cells

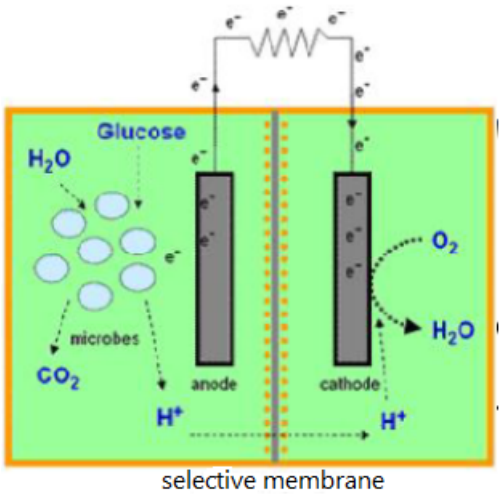

Figure 1.4: Block diagram of Microbial Fuel Cell [22]

In these fuel cells bacteria is used for producing electricity as it consumes the wastes which are soluble in water such as alcohols, sugars, and starch etc. This property of bacteria becomes helpful in converting energy from the waste. This technology will convert the chemical stored in the domestic or industrial waste. The transfer of electrons from the bacteria to the anode of the fuel cell plays an important role in the conduction. The water waste has a certain chemical energy stored in the organic molecules which releases when these organic molecules break in to the simpler ones (e.g CO_2 etc).

Carbon nanotubes (CNT) are very famous for their mechanical properties and good surface area,

in addition they are also suitable for cell growth, electrodes of microbial fuel cells. The three dimensional architecture and the enlarged surface area of the electrodes for the growth medium will cause bacteria to grow but get immobilized. The CNT's scaffold may offer self supporting structure with large surface area through which hydrogen producing bacteria can finally grow and proliferate. Also nanotubes and MWCNTs have been reported to be bio-compatible for different eukaryotic cells.

1.5.2 Catalysts

Larger surface area is a speciality of the nanomaterials so nano catalysts have an exceptional surface activity. Nano crystalline aluminium is getting used as solid fuel for the propulsion of rockets due to its high reaction rate on the other side the aluminum in the bulk form is used in making utensils. Nano Aluminium is highly reactive and provides the needed boost to send load wage in the space. Actually, catalysts assist or delay reaction rates depending upon the activity of the surface, and they may very well be used in manipulating the rate-controlling step.

1.5.3 Television Displays

The resolution of television (TV) or computer's monitor depends upon the size of the pixels. Mainly these pixels are made of materials called "phosphorous" that light up when hit by an electron from the cathode ray tube. The improvement in display comes from the reduction in the size of the pixels, so nano crystalline cadmium sulfide, lead telluride and zinc sulfide prepared by the sol-gel method are the appropriate candidates for the improvement of the resolution. The use of nanophosphorous reduces the cost of these screens for having high definition display.

1.5.4 Microelectronics

The micro electronic industry has focused on miniaturization, so that the circuit elements such as capacitors, transistors should be small in size. By having achieved a sufficient reduction in size CPU containing such components can run much faster and allow calculations at much higher speed. However there are several barriers to such progress including the lack of ultra fine precursor for the manufacturing of these components, improper dissipation of the tremendous heat generated by these microprocessors due to high speeds, short average time to failure (unreliability). Nanomaterials are helping the industry to break down these barriers because of their ultra fine purity, better thermal conductivity durable interconnection and long lasting.

Transistors are too small to reduce the size of the subsets of electronic systems and to make smaller devices, but it is very difficult to form high quality junctions in these transistors. In particular,

for material distance less about 10 nm it is very difficult to change the doping concentration of a material. The researchers have been able to make the junction less transistors with nearly identical properties [23].

They run faster and consume less energy than any transistor in the market today. It consist of a silicon nanowire in which current is controlled by a silicon gate separated by a thin insulating layer. The silicon nanowire is n type while the silicon gate act as a p type material. The device has almost ideal electrical properties and work as the most perfect transistor without suffering from leakage current.

1.5.5 Pollution Control

Nanomaterials have large grain boundaries as compare to grain size. That's why they are very active in terms of physical, chemical and mechanical properties. Because of their high reactivity nanomaterials can be used to instantly react with the poisonous gases such as nitrogen oxide, carbon monoxide.

1.5.6 Sun Screens

Exposure of human skin in sunlight for a long time can cause severe problems. Sun screens contain nano TiO_2 which provide a high sun protection factor (SPF). They just sit on the skin to protect rather than penetrating in the skin. The sun screens containing the above mentioned nano particles block the harmful UV radiations from the sun for long time. These lotions are transparent which is also one of the advantage of these materials.

1.6 Fabrication Methods

The methods of the fabrication of nano materials can be divided in two groups; top down methods and bottom up methods. In the top down approach the nanomaterials are prepared from the bulk substrate by progressive removal. While the bottom down approach is completely opposite, in which we assemble the desired nano material starting from the atomic or molecular precursors. The both methods requires control on fabrication(e.g temperature or energy of the beam used in lithography) and environmental conditions (e.g dust, humidity). This is because nano technology needs sophisticated environment.

1.6.1 Top Down Approach

There are so many methods which are in use for this approach and we can collectively name them as "Lithography". This technique has derived from the semiconductor industry, in start we were able to separate only a piece of material in microns from the bulk using this technique. Nowadays, advancements in the lithographic techniques have made us to have a material in nano range. Some of the techniques are as under

- Photolithography
- Scanning Lithography
- Soft Lithography
- Nano contact printing
- Colloidal lithography
- Scanning probe lithography
- Nano sphere lithography

There are so many techniques under this umbrella which have proved useful but we are going to discuss very few of them briefly.

Photolithography

This technique use UV or X rays. A radiation sensitive layer is deposited on the substrate of the material and then it is exposed to light through a mask(projection mode lithography). The area which get exposed to the radiation selectively removes and it is done by placing the mask in contact with the layer(contact mode lithography). The resolution of the photo lithography (contact mode) is less because we cannot achieve the gap between the mask shorter than $1\ \mu m$. So to produce high resolution patterns we use advance photo lithographic techniques.

Scanning Lithography

In this technique highly energetic ions and electrons are used to form pattern on the radiation sensitive layer. This technique has a high resolution in the range of nanometers. When we use electrons beam in this technique it is termed as electron beam lithography and if we use ions then the technique is named as focused ion beam lithography. In case of electron beam the resolution is

near 50 nm. The focused ion beam lithography use usually ions of hydrogen, helium, lithium and beryllium and this technique has resolution smaller than that of the photo lithography. But the problem with both of these techniques is, they are serial and consequently they are very slow.

Soft Lithography

Soft lithography is a collective name for a number of techniques. In general, we prepare a mold by casting a liquid polymer on a rigid base called as master in this technique. This method is very useful and is getting used in making structure ranges from microns to nanometers with equipment which is easy to handle as compared to the lithography technique. There are so many polymers which are in use for making molds but polydimethylsiloxane is used mostly because of its non toxic nature and importance in the field of bio technology. Once we get the mold of the polymer having desired shape then we can easily use this stamp to write the desired pattern of the material that we need.

Nanocontact printing

The soft lithography technique can write the patterns of lateral dimensions $\geq$500 nm. Actually the stamp we usually use in soft lithography is highly compressible and soft as a result it gets deformed. So, to work in high resolution we need to make a more reliable stamp and the recent advancements in this technique have got the idea to make it more useful by changing the chemical composition of the stamp or placing the stamp on some other material. As a consequence of this progress now we are capable of growing nano structures of up to 50 nm by this cheaper technique.

1.6.2 Bottom up approach

The bottom up approach can be sub divided in two phases; gas and liquid. Gas phase includes plasma arcing and vapor deposition while the liquid phase bottom up approach includes sol gel synthesis and molecular self assembly.

Plasma Arcing

This is the method we use to fabricate nanotubes. In this method an ionized gas (plasma) is created between two electrodes because of the potential difference at them. The arcing device is made up of the two electrodes. The anode vaporizes as the electrons from it move toward cathode because of potential difference and these positively charged ions move from anode to cathode to pick the lost electrons and get deposited there. This technique can also be use to place nanolayers on surfaces. This deposited layer can be as thin as 1nm just near to atomic size.

Chemical vapor deposition

In this technique material to be deposited is first converted in to gas and then allow to deposit on the desired solid surface. This method is usually used to make carbides of metals and oxides, even this method can be used to make nano powder of pure metal.

Sol Gel Synthesis

Sol gel synthesis is a wet technique. It is the most useful technique and by using this we can prepare nano particles, nano structured 2D sheets and the 3D nano structured material. In sol-gel synthesis we first prepare a colloidal suspension for this sol precursors are usually used in the form of metal ions. Metal alkooxides are the most important precursors because of their readial hydrolysis. Alkooxides such as titnates, aluminates and borates can also be used as precursor. If hydrolysis of precursor is not possible because of their immiscibility in water, a mutual solvent (an alcohol) is used to do so. The sol-gel method comprise of four steps

- firstly hydrolysis of the precursor is done.Most of the times hydrolysis need no catalyst but few times basic medium (NH_3 or NaOH) or acidic medium (CH_3COOH or HF) is used as catalyst.
- Sol will then start to condense.
- As the sol is getting condensed the particles stats to grow which depends on various parameters such as temperature, PH of the sol and pressure etc
- When particles form they start doing agglomeration. The whole liquid get networked and a gel is formed.

Chapter 2

Literature Survey

2.1 Rare Earth Elements

The rare earth elements have very unique properties and they consider to be non toxic [25]. Their emission spectrum lies in ultraviolet and near infrared region and this is the reason why they considered as important candidate in field of optical fibers and lasers.

In rare earth elements the number of electron in 4f shell varies from 0 to 14 as we move from $La\ (4f^0)\ to\ Lu\ (4f^{14})$. The electronic configuration of rare earth elements is shown in fig (2.1). The

Element	Symbol	Atomic number	Electronic Configuration
Lanthanum	La	57	[Xe] $4f^0\,5d^1\,6s^2$
Cerium	Ce	58	[Xe] $4f^1\,5d^1\,6s^2$
Praseodymium	Pr	59	[Xe] $4f^3\,6s^2$
Neodymium	Nd	60	[Xe] $4f^4\,6s^2$
Promethium	Pm	61	[Xe] $4f^5\,6s^2$
Samarium	Sm	62	[Xe] $4f^6\,6s^2$
Europium	Eu	63	[Xe] $4f^7\,6s^2$
Gadolinium	Gd	64	[Xe] $4f^7\,5d^1\,6s^2$
Terbium	Tb	65	[Xe] $4f^9\,6s^2$
Dysprosium	Dy	66	[Xe] $4f^{10}\,6s^2$
Holmium	Ho	67	[Xe] $4f^{11}\,6s^2$
Erbium	Er	68	[Xe] $4f^{12}\,6s^2$
Thulium	Tm	69	[Xe] $4f^{13}\,6s^2$
Ytterbium	Yb	70	[Xe] $4f^{14}\,6s^2$
Lutetium	Lu	71	[Xe] $4f^{14}\,5d^1\,6s^2$

Figure 2.1: Electronic configuration of rare earth elements in ground state

rare earth element are commonly found as trivalent ions so the electrons in the partially filled 4f

state are shielded by the 5s and 5p orbital. In consequence, the energy levels of these ions are little affected by the surrounding environment [26].

2.2 Rare Earth Oxides

In the periodic table rare earth elements include lanthanum plus fourteen other elements. The term 'rare earth' oxide does not mean that they are rare on earth. There are rare earth elements which are in fact more abundant than copper or tin e.g Neodymium and yttrium. It is because of their extraction or purification difficulties from their ores they said to be rare earth. These elements have strong affinity with oxygen, hydrogen, carbon, silicon, nitrogen, sulphur and boron which make their purification a really challenging and tedious job. The oxides of these rare earth are hygroscopic in nature i.e, they readily absorb carbon dioxide and humidity from atmosphere. Although these oxides have unique properties but due to their demand in present technological advancements there lies a great interest for the improvement of their properties among researchers. This is due to the fact that their oxides lie in $4f^n$ electronic configuration and their ionic radius decreases as the atomic number increases exceptionaly. These RE oxides have the potential to replace SiO_2 in the integrated circuits (IC's) for their betterment.

2.2.1 Scaling of the devices

Integrated circuits have been very important in every device in our daily routine. Metal oxides Semi-conductor field effect transistors (MOSFETs) are considered as building unit of the modern technology. Electronic industry is trying to scale down devices according to Moore's law [27]. Moore's Law states that in approximately two year the number of transistors on ICs gets doubled. In other words, after two years the performance of the chip will be double.
In MOSFET's silicon dioxide is using as gate dielectric material from a long time so it has reached its critical restrictions. Materials with high dielectric constant (k) are necessary for the scaling of the devices at the current rate.

2.2.2 High ϵ Materials

To introduce a new dielectric material as replacement for silicon dioxide in ICs, materials should reach following criteria as published by International Technology road map of semi conductors (IRTS),(2009)

1. Dielectric constant of the substitute should be greater than that of amorphous SiO_2 (=3.9).

2. The Material should be thermally compatible with silicon i.e it can bear a temperature of approximately 900 ^{0}C.

3. The band gap of the material should be higher than 4 eV in order to lower the gate leakage current.

4. The material should have low electrically active defect at interface between new material and silicon.

5. The thickness of the material to be deposited as substitute to SiO_2 must be equal to the thickness of SiO_2 layer.

Silicon dioxide is losing its interest in newly developed IC's because of the increase of leakage current due to quantum tunneling effect of electrons in SiO_2. So to eliminate this problem SiO_2 is getting replaced by some other suitable materials.

2.2.3 Dielectric Constant

In order to replace SiO_2, new material should have a dielectric constant greater than 5 [28]. There is an inverse relationship between the band gap and dielectric constant. This is why materials with very high dielectric constants are not useful in Integrated circuit improvement. The Clausius Mosotti equation for dielectric constant

$$k = \frac{3V_m + 8\pi\alpha_D^T}{3V_m - 4\pi\alpha_D^T} \tag{2.1}$$

where α_D^T is the total dielectric polarizability and V_m is the molar volume. In α_D^T all types of polarizations are summed up. In MOSFETs the working frequency doesn't support dipolar or space charge polarization. So there will be no contribution of these two polarizations. V_m can be calculated by the parameters of unit cell

$$V_m = l_1 l_2 l_3 \frac{\sqrt{1 - \cos^2 a - \cos^2 b - \cos^2 c + 2\cos a.\cos b.\cos c}}{Z} \tag{2.2}$$

l_1, l_2 *and* l_3 are lengths of unit cell and a, b and c are inter axial angles while Z represent number of formula units per cell.

To find the total polarizability we will apply additive rule to sum up dielectric polarizability of all ions in a formula unit of a multi component material.

$$\alpha_D^T = \sum_{j=1}^{n} V_j \alpha_D(j) \tag{2.3}$$

n is the total number of ions and V_j is the number of ions of the type j. The static dielectric constant of oxides can be calculated by this relation

$$k = n^2 + \frac{Ne^2 {Z_T^*}^2}{m\omega_{T_0}^2} \tag{2.4}$$

where n is the refractive index and its value is 4-5 for the materials with wide band gap, N is the concentration of ions, e is the charge on electron, Z_T^* is the transverse effective charge, m is the reduced mass of ions and ω_{T_0} is the frequency of transverse optical phonon.

2.3 Dielectric Polarization

If an electric field is applied to a dielectric material it polarizes and the magnitude of bound charge density (σ_b) can be considered as dielectric polarization or in other words we can say if there are N number of dipoles existing in the dielectric material (each dipole consist of +q and -q charge separated by a distance d) in the presence of applied electric field then the dipole moment per unit volume is the dielectric polarization. If a given dielectric material has n number of atoms or molecules per unit volume and each atom or molecule is polarized then we can write

$$P = n(q \times d) = n \times \mu \tag{2.5}$$

If the total charge density for a capacitor is σ then the $\sigma - \sigma_b$ is the free charge density σ_f. This free charge density creates a flux density (D_0) using Gauss's law we can write

$$D_0 = \epsilon_0 \times E \tag{2.6}$$

The total dielectric flux density can be written as,

$$D = P + D_0 \tag{2.7}$$

The total dielectric flux density can be written as D = $\epsilon \times E$, then the above can be written as

$$P = (\epsilon - \epsilon_0)E \tag{2.8}$$

The dielectric susceptibility(χ_e) is also an important parameter which describes the relationship between the applied electric field E and the polarization P

$$P = \chi_e \epsilon_0 E \tag{2.9}$$

Dielectric susceptibility actually defines how easily the atoms in the material get polarize by an applied electric field. Now comparing equation 2.8 & 2.9 we can write

$$\chi_e = \frac{(\epsilon - \epsilon_0)}{\epsilon_0} = (\epsilon_r - 1) \tag{2.10}$$

by putting equation 2.10 in 2.9 we can write

$$P = (\epsilon_r - 1)\epsilon_0 E \tag{2.11}$$

from the above equation we can write

$$\chi_e = \frac{P}{D_0} \tag{2.12}$$

so the dielectric susceptibility is the ratio of the bound surface charge density to the free surface charge density. χ_e for the vacuum is zero because there are no atoms, molecules or ions to polarize. If the atoms or molecules of the materials are more polarizable then the bound surface charge density will be higher so as the dielectric susceptibility or dielectric constant.

2.4 Polarization Mechanisms

In this section we will discuss some mechanisms in which atoms or molecules get polarized due to electric field application.

2.4.1 Electronic Polarization

As all the materials are made up of atoms, when an electric field is applied the electronic charge of atoms shifts toward positive electrode. This small displacement occurs at very fast pace even if the applied electric field changes its polarity 10^{14} times per second this polarization mechanism follow this change in polarity and exist in the material. As the electric field of the visible light has a frequency of 10^{14} so the visible light can also interact with the material and polarize it. That is why electronic polarization also named as optical polarization.

Molecules and ions also get polarized similar to the neutral atoms. The electronic polarization of the ions is approximately the same as the atom with equivalent number of electrons e.g the electronic or optical polarization of the sodium ion Na^+ is similar to the Neon atoms. The electronic polarization has a direct relationship with the size of atoms the greater the size the higher will be the polarization. So, the polarization of anions is usually higher than that of cations because of the greater size of anions as compared to cations. The electronic polarization of the molecules is greater because of the large number of electrons in them.

2.4.2 Dipolar Polarization

Polar molecules have a permanent dipole moment and these molecules experience a torque when an external electric field is applied to these molecules. These dipole moments then align themselves in the direction of external applied field. So the bound charge density (σ_b) increases as a result

the polarization of the material increases. The dipolar polarization only occurs if the molecules of material are having permanent dipole moment. This dipolar polarization is the reason for the high dielectric constant of water molecules.

Dipole moment of the polar molecules is very large as compared to that induced by the polarization of atoms. The dielectric constant of polar molecules is usually greater. The polar molecules in the solid form are not free to move as compare to that of liquid or vapor state. In case of ice the permanent dipoles are present but they are not free to rotate as the electric field changes its polarity. So the effect of this polarization mechanism is smaller in polar solids as compared to that of polar liquids or gases.

2.4.3 Maxwell-Wagner Polarization

There are some dielectric materials which have relatively mobile ions. At higher temperatures the applied electric field cause the ions to diffuse through the interfaces (grain boundaries) and hence building a double layer capacitor at the the interfaces. The polarization due to such mobile ions in the dielectric material is termed as Maxwell-Wagner polarization.

This polarization mechanism becomes important to consider at higher temperatures because the increase in temperature causes the thermal energy of the the ions or electrons and hence the chance of diffusion increases. This polarization doesn't sustain at the high frequencies because the mobile ions cannot orient themselves too rapid.

2.5 Frequency dependence of Dielectric constant

The polarization of the dielectric medium requires the displacement of the dipoles, electronic clouds and ions. Although the displacements are very small but a finite amount of time is required to make these displacements. In the covalent bonded materials the electronic polarization establishes quickly. In these dielectric materials the change in polarity of electric field at the rate of 10^6 times per second can easily be followed. So this polarization mechanism contribute in the value of dielectric constant even at very high frequencies. Electronic polarization is the only polarization mechanism which can follow high frequencies while all other die before.

Dielectric relaxation or frequency dispersion is defined as the lowering of dielectric constant with the increase in frequency. The dielectric constant at low frequencies is also called as static dielectric constant while the dielectric constant at high frequencies is named as optical frequency dielectric constant.

2.6 Erbium Oxide

Erbium Oxide (Er_2O_3) also named as erbia has a cubic crystal structure but at high temperature its structure changes. It has a body centered cubic phase near 2320 ^oC and a hexagonal close packed structure above 2320 ^oC [29]. Erbia has a high melting point of 2430 ^oC. Each unit cell of erbia contains 80 atoms, 32 of which are erbium atoms which are located on 8b and 24d Wychoff positions, and 48 oxygen atoms sit in the 48e ($x = 0.3914,\ y = 0.1528,\ z = 0,3819$) positions [29]. Band gap of erbium oxide is approximately 5.4 eV [30]. It has unique physical and electrical properties and an extraordinary thermal and chemical stability. The mechanical properties of erbia are getting used in thermal barrier coating and also in some structural applications [31].

2.6.1 Literature Survey

The properties of nano films of erbium oxide grown on poly crystalline silicon substrate has studied at different annealing temperatures in detail [30]. In this work x ray diffraction of the films annealed at different temperatures revealed that the diffraction patterns were getting stronger with increase in annealing temperature upto 800 ^oC and the patterns started to diminish as the temperature of annealing further increased.

X ray photoelectron spectroscopy performed on the samples annealed at different temperatures showed that the peak of erbium of the sample annealed at 600 ^oC, 700 ^oC, and 800 ^oC shifted closer to that of the Er_2O_3 by 0.9 eV. The atomic force microscopy of all the samples was done and it was reported that the sample which was annealed at 800 ^oC was having more uniform surface. Furthermore, the gate voltage shift was indicated for all samples under a constant current stress. In addition the same measurements of gate voltage performed on a sample which was rapidly annealed at 800 ^oC and it was reported that this sample has a smallest shift among all the samples.

Sintering effect on structural and electrical properties of sol gel synthesized erbium oxide has been studied by A. Bakhsh et al. in 2012 [32]. The X-ray diffraction of the synthesized powder confirmed that erbium oxide has a cubic structure with a lattice constant of 10.557 and average crystallite size found to be 40 nm. The properties of the sample synthesized in laboratory compared with a sample purchased from market.

The synthesized sample sintered at 1400 ^oC was found having the average grain size b/w 150-500 nm. The dielectric constants of synthesized and purchased samples were also compared at different sintering temperatures and it was deduced that the dielectric constant decrease with increase in sintering temperature. The dissipation factor $\tan\delta$ at lower frequencies was higher for the synthesized

sample and showed a decreasing trend with increase in frequency.

Structural and electrical characterization of the films of erbium oxide grown on silicon(100) substrate by MOCVD technique has also reported in the literature [33]. The films were deposited at different temperatures from (450 ^oC to 600 ^oC) at pressure of 2 torr. X-ray patterns showed that at 500 ^oC a poor crystalline phase and more amorphous phase of erbium oxide exist. They found that the crystalline phase established in film grown at 525 ^oC or above and also discussed that erbium oxide films grown on silicon substrate depends strongly on the growth conditions. The grain in the film was found in the range 18-35 nm using Scherrer relation. The atomic force microscopy of the films revealed that as the temperature increased the roughness of the film also increased. High Capacitance voltage measurements were performed on the films and the dielectric constant was found in the range 8-10. They also reported in their work that the dielectric constant does depend upon the thickness.

V. Mikhelashvili et al. studied the structural and electrical characteristics of Er_2O_3 films that were grown by electron beam gun evaporation. They described evolution of the morphology with annealing temperature and the structure thickness. The dielectric characterization showed the dielectric constant to be in the range of 6-14. A minimum leakage current were noticed at an applied field of 10^6 V/cm and the breakdown electric field was also demonstrated. The leakage current and breakdown electric field were correlated with the surface morphology. These characterization suggested this material to be replacement for silicon dioxide as a gate dielectric [34].

M. Miritello et al. studied the structural properties and optical properties of erbium oxide thin film grown by magnetron sputtering. Annealing process was found to have beneficial effects on both the structural and optical properties. Photoluminescence intensity of the annealed films was reported 40 times greater than the intensity of as deposited samples. The increased efficiency of photon emission yielded a longer life time of the photoluminescence signals [35]. D. Levchuk et al. reported erbium oxide as a promising tritium permeation barrier. They tested thermal load and permeation measurements to check that erbium oxide is compatible with other materials at extremely high temperatures. It was found that a coating of crystalline erbium oxide of 1 μm thickness reduced the permeation by 1000 times as compared to the relevant material Eurofer 97. Furthermore, the coatings were found to have good thermo-mechanical stability on different substrates [36].

2.7 Description of Apparatus and Method for preparing Erbium Oxide

2.7.1 Description of Apparatus

For the synthesis of Erbium Oxide nanoparticles and films the following apparatus was used

- Digital Balance
- Hot Plate
- PH-Paper
- Mortar Pestle
- Die
- Hydraulic Press
- Doctor Blade Film Coater
- Tube Furnace
- Oven
- Crucible

Digital Balance

The digital balance is the most important thing while working in the laboratory. The balance was used to weigh chemicals during the preparation of the material.

Hot Plate

The hot plate is used to provide heat during reaction it may also stir the solutions. In this work the hot plate was used to stir and heat the reactants. The hot plate available in thermal transport lab SCME, can provide temperature from 0 ^oC to 300 ^oC.

PH Paper

In the sol gel process the PH of the sample should be neutral. So for noticing the PH of the reaction mixture, PH papers were used.

Die

For making pellet the die is an essential thing. They are made of very hard materials and usually available in circular shapes with a diameter from 5-15 mm. The die used in this work was having a diameter of 13 mm.

Hydraulic Press

Hydraulic press is used to apply a pressure on the material inside the die during pellet preparation. It has a pressure meter which shows the applied pressure. Some of the hydraulic press have facility of heating while pressing the sample. In making Erbium Oxide pellets only pressing was done.

Doctor Blade Coater

The doctor blade coater was used to coat films on the substrate. Doctor Blade coaters are usually available to grow films in the range of thickness in microns. In this work the coaters of 2 and 10 μm was used.

Tube Furnace

The furnace is also an important thing in nano particles synthesis and the furnace that is used to anneal or sinter the samples. The tube furnace available at the lab can heat the sample up to 1500 ^{o}C. It can create vacuum while heating but this facility was never used in the whole work.

Oven

The oven available at Thermal Transport Laboratory can heat upto 300 ^{o}C on maximum. The oven was used to provide constant heat to the samples while drying. The oven was very useful in drying the apparatus after washing or rinsing. The same oven was used in measurements of resistivity of the pellet by two probe technique.

Crucible

The crucibles are usually made of ceramic and used to heat the samples. They have very high melting point so that they do not melt while heating samples in them. The boats and beakers were used in this work.

2.8 Synthesis of Erbium Oxide

In few decades the sol gel process has attracted a tremendous international interest, because of its potential in modification and improvement of materials. The Sol-Gel process was used to prepare Erbium Oxide from its nitrate precursor. The Erbium Nitrate pentahydrate purchased from Sigma Aldrich of purity 99.99 percent was used in this synthesis. The all other chemicals were used of research grade in this synthesis.

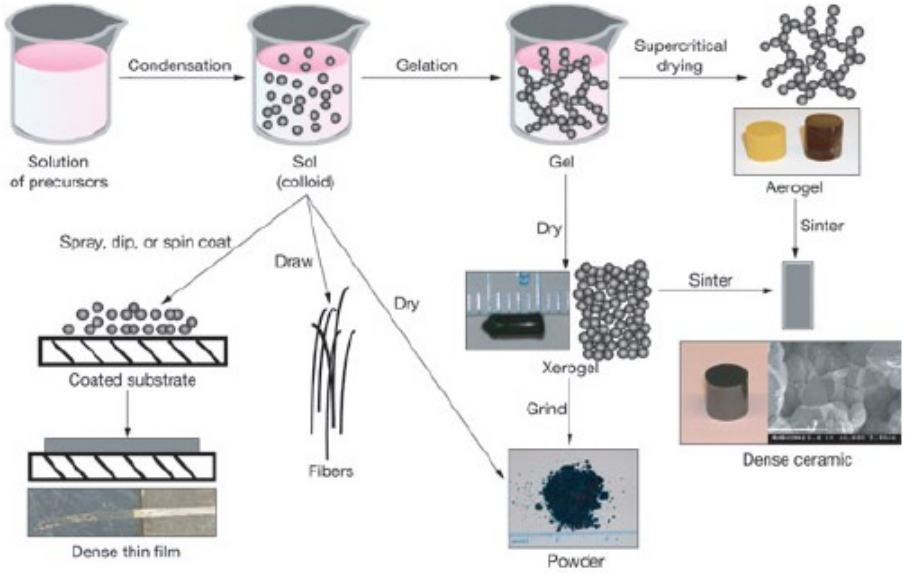

Figure 2.2: Flow Diagram of Sol-Gel synthesis [37]

To prepare Erbium oxide firstly 0.02 moles of erbium nitrate pentahydrate were dissolved in 10 ml of ethanol. In another beaker 5 ml of ammonia was dissolved in 10 ml of ethanol. The two mixtures were then mixed together to form a sol. The PH of the sol was monitored using PH paper and it was kept to a better electrophoretic stability. Then a little drop of this sol was spread using doctor blade on a silicon substrate Si(100). The doctor blade for different thickness of the films was used. The films and the sol in the beaker was then dried completely at 50 ^{o}C. These dried samples were then annealed at different temperatures. Sample in the form of powder was heated in boats while the films on the Si(100) substrates at the pace of 10 ^{o}C per minute in a tube furnace. After their annealing they were slowly cooled at the rate of 5 ^{o}C per minute.

Chapter 3

Experimental setup and measurements

3.1 Introduction

After preparing the required sample of (Er_2O_3) in the lab the next goal was to characterize the prepared sample. For the characterization of the material different apparatuses were used. Each characterization was revealing different information about the material e.g, physical, morphological or chemical properties. Each apparatus was working on some specific principle and in this chapter a brief introduction of these systems is going to be explained. The major measurements performed on the sample are

- X-ray Diffraction (XRD)
- Scanning Electron Microscopy (SEM)
- DC electrical resistivity measurements
- Hall Effect measurements
- Fourier Transform Infrared Spectroscopy (FTIR)
- BET Surface area
- Atomic Force Microscopy (AFM)

3.2 X-ray Crystallography

Electromagnetic radiations is among one of the great phenomena of physics and in the early part of last century science were making every effort to explore all the its detail e.g, frequency, wavelength, speed, color (if it had) and energy. When x-rays came along then these specific electromagnetic radiations become special due to their method of production. The x-rays are usually generated

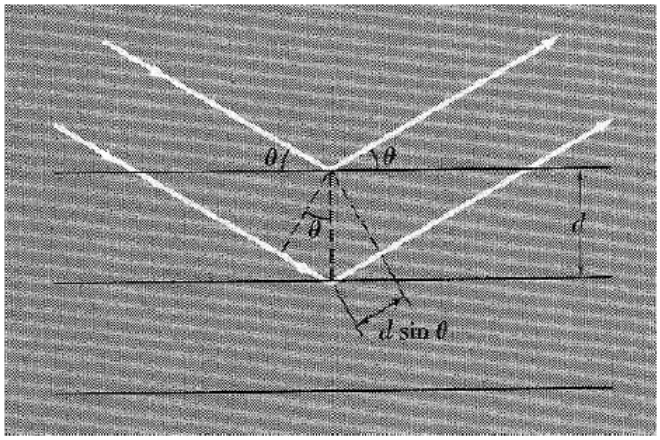

Figure 3.1: Braggs Condition and atomic planes [38]

in the cathode ray tube, to produce them we need a source of electron (a heated filament) and a high potential to accelerate these electrons. When these highly energetic electrons collide with the metal target then the target act as the source of electromagnetic radiations. These electromagnetic radiations named as x-rays. X-ray diffraction is the most useful technique to identify the crystallinity of the material. This technique nondestructively characterize the crystal structures of the powder as well as bulk material. It is the most important and commonly used technique in materials science.

3.2.1 Bragg's Law

As x-rays are the electromagnetic radiations so they can diffract and interfere like waves. While crystals can be considered as series of atoms placed in the lattice. According to W.L.Bragg explanation, the parallel planes in the crystals can be considered as partially silvered mirror and when electromagnetic waves fall on them the incident waves get partially reflected from each of these. If these reflected radiations interfere constructively only then we find diffracted beam. Now consider the planes shown in fig 3.1 each is separated by a distance'd' from the nearby plane. As x-rays fall on this arrangement of planes these rays will reflect from the adjacent planes. The reflected rays from adjacent planes will only interfere constructively if

$$2d\sin\theta = n\lambda \tag{3.1}$$

This is called the Bragg's law [38]. This law is valid if the wavelength of the radiations is comparable to the inter planar spacing or ($\lambda \leq 2d$). These reflected radiation are carrying information about the crystalline structure of the material they get reflected from.

Determination of particle size

Powder method was used in the x-ray characterization of the prepared erbium oxide. This method is the most reliable and useful because it doesn't need single crystal it requires only the powder of the sample material. Powder is used to rotate while exposing to x-rays and the diffracted beams give us peaks. The Scherrer's formula can be used to reveal the information about the particle size.

$$t = \frac{0.9\lambda}{\beta \cos\theta} \tag{3.2}$$

where the β is the full width half maximum of the peak and λ is the wavelength of the incident x-ray beam.

3.2.2 Scanning Electron Microscopy (SEM)

The scanning electron microscope is a special type of electron microscope which uses the highly focused electron beam for the sample's surface topography [39]. The electrons of the incident beam interact with the electrons of the sample and create signals which contains information about its surface morphology. There are two main goals of SEM

- Focusing the small beam of electron
- Detecting the sample interacted beam

For the first goal we need a knowledge of electron gun, apertures, condenser lens, Deflection or raster coils and objective lens.

An electron gun is the actual source of electrons it uses a thermionic emission of electrons. A thermionic gun usually uses a tungsten filament across which a voltage is applied, as a consequence of which electrons and photons emit. A field emission gun operates by having a potential difference between the filament tip and first standard. The potential difference at the second standard determine the accelerating voltage of the gun.

Apertures are the very small discs having a micron size hole in it, these apertures control size of the beam. The very important parameters are controlled by these apertures e.g, resolution and depth of focus.

The condenser lens is an electromagnetic lens. This lens is hollow in between and a current pass through it which produces a magnetic field in the center. The strength of this lens can be altered by changing the amount of current flowing through it. This lens deshapes the electron beam which doesn't effect magnification it simply changes the focus and fine adjustment of the beam is done through this lens. The condenser in the last converge the beam in to a fine beam like that which

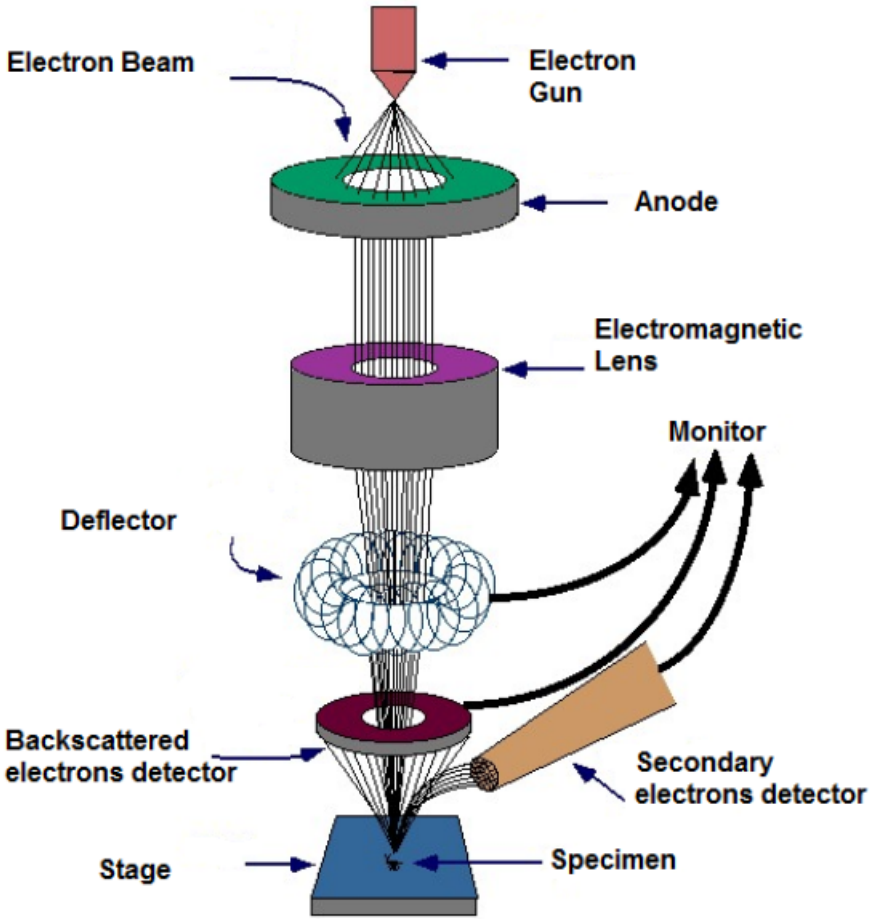

Figure 3.2: Scanning Electron Microscope block diagram [41]

emitted from the gun. Increasing the magnification is nothing than decreasing the size or area over which electron beam travel.

The deflector deflects the beam in various different x,y directions so that the beam sweep over certain area of the sample. It can move the beam from left to right and top to bottom.
The electron beam from the deflector then enters in objective lens which converge it into fine beam. And this fine electron beam is focused on the sample by the objective lens.
When electron beam comes out of the objective it interact with the sample. And the following phenomena takes place

- Emission of secondary electrons
- Emission of back scattered electrons
- Emission of X-rays

- Electrons back scattered diffraction

There are so many modes in which SEM can operate. The selection of operating mode depends upon the sample and feature we need to study. The two modes are breifly explained here

Secondary electron mode:

When the electron beam interact with the sample it knock out electrons from the specimen's upper 5 nm layer. Those electrons having energy between (0-30 eV) detected by the detector and help in making image.

Back Scattered e.beam:

Those electrons in the beam which bounce back from the specimen elastically are detected in this mode and help in making the image. The energy of these electrons typically lies between 15-30 keV.

3.2.3 Energy Dispersive X-ray Spectroscopy

Energy dispersive X-ray spectroscopy (EDX or EDS) is a technique used for the elemental analysis in combination with scanning electron microscopy (SEM). It detects the x-rays emitted by the sample when exposed to electron beam to characterize the elemental composition of the sample being exposed. When the sample gets bombarded with the electron beam of the SEM the electrons of the sample get excited and eject out from the atoms constituting the surface of the sample. In consequence the electrons from the higher energy levels move down to fill the resulting vacancy. As the electrons move from higher energy level to the lower energy level they emit radiations in the form of x-rays to balance the energy difference between two states. The energy of x-rays is characteristic of the element they get emitted from.
The EDS detector is used to measure the relative abundance of these x-rays versus their energy. When the the emitted x-ray strike with the detector it gives rise to a charge pulse which depends upon the energy of the x-rays, this charge pulse then converts into voltage pulse by a charge sensitive pre-amplifier. The signal then sent to multichannel to sort the pulses by the voltage. The energy determined from the voltage versus counts spectrum then displayed on screen of a computer.

3.2.4 Fourier Transform Infrared Spectroscopy

It is an important technique in the field of organic chemistry to identify different functional groups in the molecules of sample. Also, fingerprint region (1-1000 cm) can be compared with that of pure

compound to identify its identity. A source is used to generate light; all the energy of the source falls on to the sample after passing through an interferometer.

Firstly, as the source generates light it sends all of the light to the interferometer. In interferometer

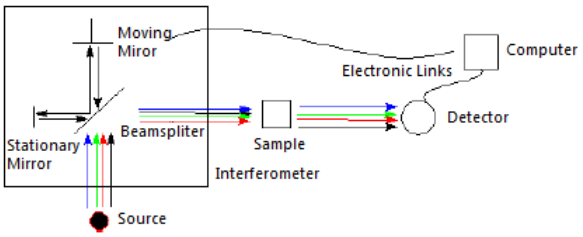

Figure 3.3: FTIR Setup [42]

a beam splitter splits the light in two direction which are at right angle to each other. One beam from the splitter strikes with a fixed or stationary mirror while the other one with a moveable mirror, and then both beams reflect back to beam splitter. The moveable mirror variate the path length between the two beams and as a result of which constructive and destructive interference take place at beam splitter. The recombined beam pass through the sample and sample absorb the certain characteristic wavelength of its spectrum. The detector then record the energy versus time data for all the wavelengths. To convert energy versus time graph into intensity versus frequency spectrum, we use fourier transform.

$$F(r) = \sum T(k) \exp(-2\pi \frac{\imath rk}{N}) \tag{3.3}$$

T(k)and F(r) are time domain and frequency domain respectively. This work can easily be done by even a slow computer [42].

3.2.5 Hall effect

This effect was first discovered by E.H Hall in 1879. Consider a sample such that a magnetic field is pointing through the sample in x direction and a current is flowing through the sample in y direction. The free charge carriers (electrons or holes) will experience a Lorentz force

$$\vec{F} = q(\vec{v} \times \vec{B}) \tag{3.4}$$

where

q$\longrightarrow$ charge of the carrier.

v$\longrightarrow$ velocity of the carrier.

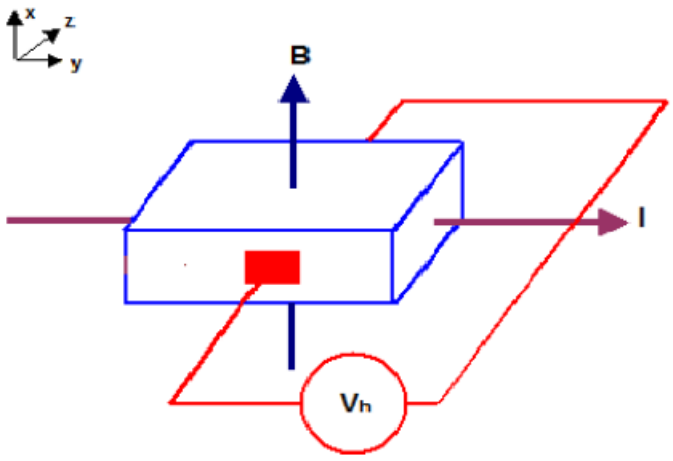

Figure 3.4: Block diagram of the hall effect

B⟶ magnetic field strength. This lorentz force on the charge carriers will deflect them in the positive z direction. If the charge carriers are electrons then a negative charge will accumulate on the +z edge of the sample on contrary if the charge carriers were holes then a positive charge would accumulate on this side. The distribution of the charges will produce an electric field in the y axis which

- Balances the Lorentz force on the charge carriers which are moving in the z direction.
- Creates a voltage difference

$$V_H = wE_H \tag{3.5}$$

  where w is the width of the sample.

When the electric field balances the Lorentz force on the carriers we can write

$$\vec{F} = q(\vec{v} \times \vec{B} + \vec{E}) = 0 \tag{3.6}$$

$$\Rightarrow \vec{E} + (\vec{v} \times \vec{B}) = 0 \tag{3.7}$$

$$E_H = v_y \times B_x \tag{3.8}$$

The sign of the Hall voltage define the type of semiconductor material if it is positive then material will be p type and for n type semiconductor the hall voltage appears negative.
The total current I which is passing through the sample can be written as

$$I = J\omega t \tag{3.9}$$

where J is the current density and t is the thickness of the sample.

$$I = (-envv_y)\omega t \tag{3.10}$$

By substituting 3.10in 3.5 we get

$$V_H = -\frac{I_y B_x}{ent} \tag{3.11}$$

Now the hall coefficient which is defined as

$$R_H = \frac{E_H}{J_y B_x} \tag{3.12}$$

which can be simplified as

$$R_H = -\frac{1}{en} \tag{3.13}$$

where e is positive by definition. Now for the positive charge carriers or the p-type semiconductor the hall voltage can be written as

$$V_H = \frac{I_y B_x}{ent} \tag{3.14}$$

and the hall coefficient will become

$$R_H = \frac{1}{ep} \tag{3.15}$$

where e is positive by definition.

3.2.6 Methods for Resistivity measurements

In nanomaterials resistivity of the material is different from that of the bulk. The total resistivity a material offers usually divided into three contributions from resistivity of impurities, resistivity of grain boundaries, and the resistivity of the defects in the crystal. The electrical resistivity can be considered as proportional to the mean free path between collisions as the path increases resistivity also increase. Size reduction has two effects on material resistivity. Firstly the reduction of the size decreases the defects hence the scattering through the defects also decrease as a result of which resistivity decrease. As the scattering through the defects cause a little increment in the resistance that's why at room temperature the resistivity of the sample reduced by a small unnoticed value. While there is a contribution in resistivity due to surface scattering as the size decreases. In 2D and 1D nanomaterials this surface scattering cause the resistivity to increase [40]. To measure the resistivity of the materials usually these two fundamental methods are used

1. Two Probe Method
2. Four Probe Method

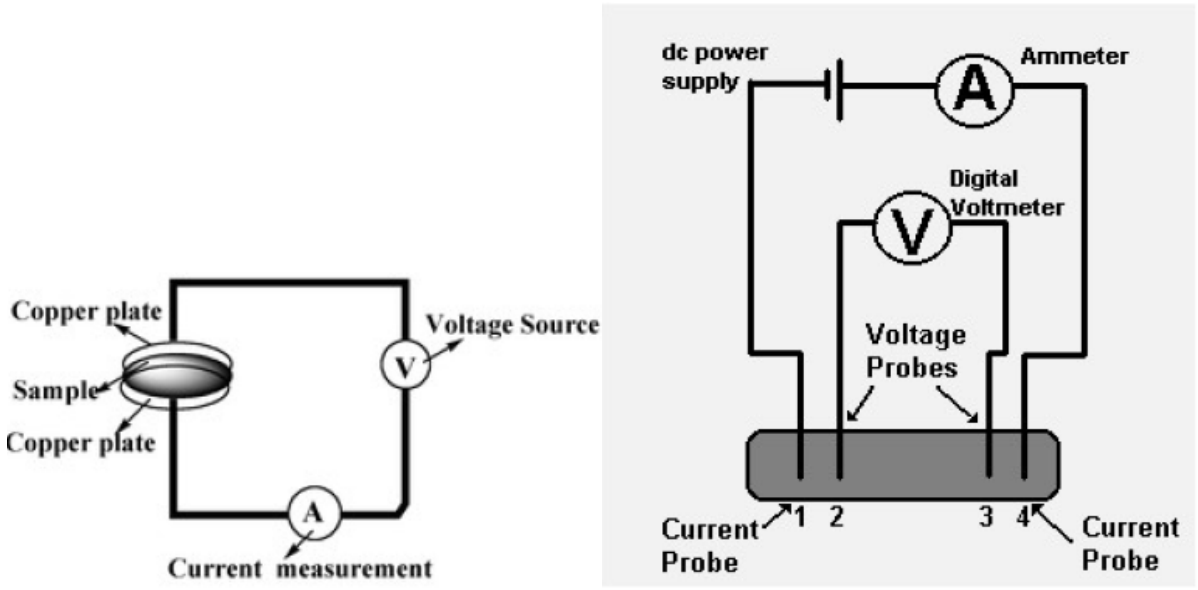

(a) (b)

Figure 3.5: Block diagram of (a) Two Probe Method, (b) Four Probe Method

Two Probe Method

In this method we apply a known voltage to the sample and measure the resulting current. The shape of the sample is important parameter in two probe method; disc, parallelepiped, cube and cylinders are acceptable shapes for this method. Depending up on the resistance sample offers Galvanometers, Ammeter, mili or micro meters and electrometers can be used to measure the current. In this method the sample is placed inside two symmetrical electrodes. As we change the voltage across the sample a different current flows through it and from the values of current and applied voltage we can easily find mean resistance from the slope of the voltage versus current graph. This method is an easy and cheap but has few limitations and errors. The main problem is the voltage drop across the sample electrode contact resistance and this method can only be applied on sample having above defined shapes.

Four Probe Technique

The four probe technique as name indicates consist of four electrodes of tungsten with small diameter of contact points. These four probes are usually placed linearly on the sample. A constant current source is connected to the outer two electrodes and a high inner impedance voltmeter is connected across the electrodes in between. A current is caused to flow through the two outer electrodes while the inner two electrodes draws no current because of the voltmeter having high inner resistance in

the circuit. So in this method we succeeded in getting rid of the unwanted voltage at the contact of sample and electrode. The resistivity of the sample can be found by using the relation,

$$\rho = \frac{\rho_0}{f(w/d)} \tag{3.16}$$

where $\rho_0 = \frac{V}{I}\ (2\pi d)$, w is the width of the sample and d is the separation between the electrodes.

3.2.7 BET Equation for Specific Area Measurement

Brunauer-Emmett and Teller introduced an important technique to measure specific surface area in 1938. The method was named BET, and this abbreviation consists of the first initial of their family names. With the help of this method isothermal derivation can be carried for the multimolecular adsorption. Let us consider $s_o,\ s_1,\ s_2,$ ... be the specific surface area covered by 0,1,2, ... layers. At equilibrium s_o remains constant, and the rate of evaporation from the first layer equals the rate of condensation on the bare surface.

$$a_1 p s_o \ = \ b_1 s_1 e^{(\frac{-E_1}{RT})} \tag{3.17}$$

where p is the pressure, and E_1 is the latent heat of adsorption for the first layer. While $a_1,\ and\ b_1$ are constants. At equilibrium s_1 should also remain constant so, there are four different ways in which it can change (a) by condensation on the first layer, (b) by the condensation on the bare surface, (c) by evaporation from the first layer (d) by the evaporation from the second layer. So,

$$a_2 p s_1 - a_1 p s_o \ = \ b_2 s_2 e^{(\frac{-E_2}{RT})} - b_1 s_1^{(\frac{-E_1}{RT})} \tag{3.18}$$

using equation 3.17

$$a_2 p s_1 \ = \ b_2 s_2 e^{(\frac{-E_2}{RT})} \tag{3.19}$$

so we can say that the rate of evaporation the second layer is equal to the rate of condensation on the first layer top. The total surface area can be written as

$$A \ = \ \sum_{i=0}^{\infty} s_i \tag{3.20}$$

and the total adsorbed volume is

$$v = v_o \sum_{i=0}^{\infty} i s_i \tag{3.21}$$

where v_0 is the adsorbed volume per cm^2. Now we can write

$$\frac{v}{A v_o} \ = \ \frac{v}{v_m} \ = \ \frac{\sum_{i=0}^{\infty} i s_i}{\sum_{i=0}^{\infty} s_i} \tag{3.22}$$

The above summation can easily be solved by assuming $E_1 = E_2 = ... = E_i$ and $\frac{b_2}{a_2} = \frac{b_3}{a_3} = \frac{b_4}{a_4} ... =$ g

Now we can write,

$$s_1 \;=\; ys_o \qquad where\; y \;=\; \frac{a_1}{b_1} pe^{(\frac{E_1}{RT})} \tag{3.23}$$

$$s_1 \;=\; xs_1 \qquad where\; x \;=\; \frac{p}{g} pe^{(\frac{E_L}{RT})} \tag{3.24}$$

$$s_i \;=\; xs_{i-1} \;=\; x^{i-1}\, s_1 \;=\; yx^{i-1}\, s_o \;=\; cx^i s_o \tag{3.25}$$

where c = y/x. Now putting these results in equation 3.22 we get,

$$\frac{v}{v_m} \;=\; \frac{cs_o \;\sum_{i=1}^{\infty} ix^i}{s_o[1 \;+\; c\sum_{i=1}^{\infty} x^i]} \tag{3.26}$$

The numerator and denominator are merely geometric progression and can be solved easily. So by simplification we found,

$$\frac{v}{v_m} \;=\; \frac{cx}{(1-x)(1-x+cx)} \tag{3.27}$$

At p = p_o the volume will get infinite so x in the equation 3.24 will be unity. So by substituting it in equation 3.27 we get

$$v \;=\; \frac{v_m cp}{(p_o - p)[1 \;+\; (c-1)p]} \tag{3.28}$$

for p $\ll$ p_o the above equation can be written as [43]

$$\frac{p}{v(p_o - 1)} \;=\; \frac{1}{v_m c} \;+\; \frac{(c-1)}{v_m c}\frac{p}{p_o} \tag{3.29}$$

Chapter 4

Results and Discussion

4.1 Introduction

Erbium oxide(erbia) was first prepared in pure form by C. James and J. Urbain [44] in 1905. It has a cubic structure but its structure has temperature dependence; it shows a body centered cubic structure near 2300 ^{o}C and a hexagonal closed packed structure above 2320 ^{o}C [29]. Erbia is inert with many liquid metals so it is a useful corrosion-resistant material [45]. It is chemically and thermally stable and finds its application in DEMO reactors [46–49], as a permeable barrier for the isotopes of hydrogen in the operational range of temperature. The presence of intermediate energy levels in Er_2O_3 make it very useful in upconversion of optoelectronic processes [50]. Some work has been done on this material but still there is need to explore its more interesting properties. Electrical, optical and photoluminescence properties of erbium oxide make it very special for many applications. The researchers have great interest in doping different materials with Er^{3+} because of their size dependent electrical and optical properties [51]. Amongst rare earth oxides it is the most important candidate in biomedical usage. The nanoparticles of erbium oxide are found very helpful in bio imaging [51]. It has also been found its uses in the coloring of glasses because of their photoluminescence [52].

4.2 X-ray patterns

In order to reveal information about the structure of the Erbium Oxide synthesized in the laboratory, x-rays diffraction of the powder was done. The best temperature for annealing of the sample was also found on the basis of its structure and grain size. Fig 4.1 shows the X ray diffraction pattern of the erbium oxide in powder form annealed at 600 ^{o}C and 400 ^{o}C for 45 minutes. The diffraction pattern of the synthesized erbium oxide was found in agreement with that reported in literature [53]. The broadness of peaks suggested that the dimensions of particles are in the nanometers. With the

help of these patterns the lattice constant 'a' of the Er_2O_3 was calculated and it was found that the the synthesized erbium oxide was having a cubic structure. In this analysis Copper k_α X-rays of

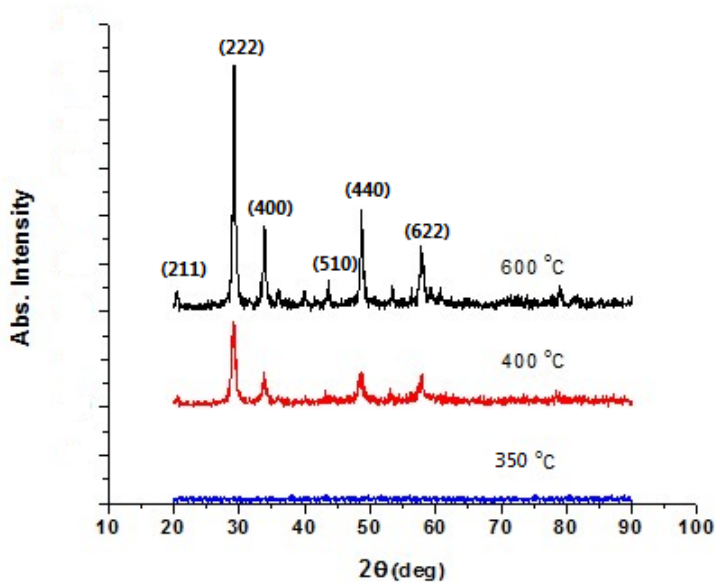

Figure 4.1: X-ray diffraction pattern of Erbium oxide(powder) annealed at 350 ^{o}C, 400 ^{o}C and 600 ^{o}C

wavelength $\lambda =$ 1.5406 Å was used. It was also found that at temperature below 400 ^{o}C the material was amorphous and no peak appeared in the diffraction pattern of the sample annealed at 350 ^{o}C. At annealing temperature near 400 ^{0}C crystalline phase started to establish in the material. The X-ray diffraction pattern of the sample treated at the 400 ^{o}C for 45 minute is shown in fig 4.1. As the average crystallite size is inversely proportional to that of the broadness or full width half maximum (FWHM), so the sample annealed at 400 ^{o}C shows that the crystallite size is smaller as compared to that of the sample sintered at 600 ^{o}C. But the sample is less crystalline and having amorphous phase in it at 400 ^{0}C. The further increase in temperature caused the grain size to increase further. As the purpose of this research was to synthesize nanoparticles of Er_2O_3 so we chose the sample annealed at temperature 600 ^{0}C for further characterization.

4.2.1 Structural Analysis of the prepared Er_2O_3

The structural analysis involving calculation of lattice parameter (a), porosity (P), bulk density (ρ_b), XRD density (ρ_X) and surface area (S) of the annealed sample of erbium oxide was performed on X-Ray diffraction patterns. In the diffraction pattern strong beams appear when the Bragg's

condition satisfy:

$$n\lambda = 2d\sin\theta \tag{4.1}$$

where n is the diffraction order and it usually taken as 1, λ is the wavelength of the X rays incident on the sample and 'd' is the planar spacing. In the cubic structure the planar spacing and lattice constant are related by the following relation:

$$a = d_{hkl}\sqrt{h^2 + k^2 + l^2} \tag{4.2}$$

where h,k and l are the Miller indices. Combining equation 4.1 and equation 4.2 we get

$$a = \frac{\lambda\sqrt{h^2 + k^2 + l^2}}{2\sin\theta} \tag{4.3}$$

Thus for all sets of the Miller indices there will be an angle which satisfies Bragg's condition such that the value of $\frac{\lambda}{2a}$ will remain constant [54].

The lattice parameter was found to be 10.558 Å and the value was in agreement with the published results of erbium oxide [32, 55].

The X-ray density of the sample can be calculated using the following equation

$$\rho_x = \frac{16M}{N_a a^3} \tag{4.4}$$

M denotes the molecular mass of the sample, N_a is Avogadro's number. As the powder was compressed into cylindrical pellet under 5ton pressure. So the bulk density of the system can be found using following equation:

$$\rho_b = \frac{m}{\pi r^2 h} \tag{4.5}$$

where $\pi r^2 h$ is the volume of the cylindrical pellet of radius 'r' and mass 'm'. The bulk density for the erbium oxide annealed at 600 ^oC was found to be 5.29 g/cm^3. Now the porosity of the material can be found easily using formula [57],

$$P = 1 - \frac{\rho_b}{\rho_x} \tag{4.6}$$

And the porosity was found 0.38. Actually the theoretical density is always greater than density of the bulk because mere pressing cannot make the material to get as aligned as in a crystal and because of this materials have porosity in them. XRD helps to estimate the surface area of the sample [56]. For spherical crystallites the number of particles can be calculated using a simple formula

$$N = \frac{Volume\ of\ 1\ gram}{\frac{4}{3}\ \pi\ (1/2\ the\ avg\ crystallite\ size)^3} \tag{4.7}$$

where N is the number of particles in one gram of the material. Volume of 1 gram was found using equation 4.4. The surface area was then calculated using this relation

$$s = N.(4\pi r^2) \tag{4.8}$$

where r is the 1/2 of the average crystallite size. The system international units of specific surface area are m^2g^{-1}.

Table 4.1: **Structural Analysis using XRD results**

Annealing Temp.(^{o}C)	**a** (Å)	ρ (g/cm^3)	**s** (m^2/g)	**t** (nm)
400	10.558	8.64	30.19	23
600	10.558	8.64	19.99	34

4.3 Brunauer, Emmett and Teller Analysis of Surface Area

Stephen Brunauer, P.H. Emmet and Edward Teller in 1938, for the first time found a method to measure the specific surface area of the finely divided and porous solids. When a gas is brought into contact with solid, some of the gas is taken up by the surface of the solid and it remains there. In this physical adsorption a weak Vander waal force of attraction between the surface of the solid and the gas molecules exist. They found this adsorption as a useful tool to explain surface area, pore volume and pore size distribution. Brunauer, Emmett and Teller introduced an equation to find the surface area which is

$$\frac{1}{[W_a(\frac{P_0}{P}-1)]} = \frac{C-1}{W_m C} \times \frac{P}{P_0} + \frac{1}{W_m C} \tag{4.9}$$

where P is the partial pressure of the gas in equilibrium with the surface of the solid, P_0 is the saturated pressure of the gas, $W_a$is the weight of gas adsorbed at STP, $W_m$is the weight of gas to adsorb a monolayer at STP, C is a dimensionless constant related to the enthalpy of adsorption of the gas. The plot of the equation 4.9 for the experimental data of erbium oxide sample is shown in fig 4.2 The total surface area can then be written as

$$S = \frac{W_m N_a A_{ACS}}{M}, \tag{4.10}$$

where M is the molecular mass of the adsorbate,A_{ACS} is the cross sectional area of adsorbate and N_a is the Avogadro's number. The specific surface area can be found using

$$s = S/w \tag{4.11}$$

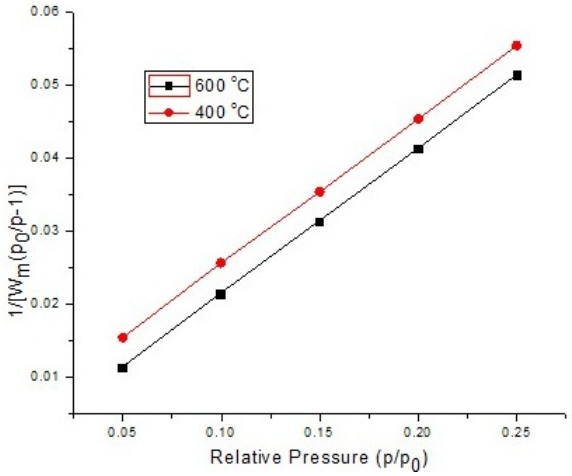

Figure 4.2: The plot of eq 4.9 for experimental data of erbium oxide

where w is the sample weight. Using these equations and doing a little calculations the surface area of both the samples were calculated and is reported in table 4.2. This result is also in agreement with surface area calculated theoretically using the XRD patterns. This point explained the power of the X-ray diffraction in material characterization.

Table 4.2: **BET surface area of the nanoparticles annealed at different temperatures and their comparison with the area found using XRD results**

Annealing Temp.(^{o}C)	$\mathbf{s}_{bet}$ (m^2/g)	$\mathbf{s}_{xrd}$ (m^2/g)	% Error
400	31.46	30.19	4.03
600	21.61	19.99	7.40

4.4 Fourier Transform Infrared Spectroscopy(FTIR)

The sample for this fourier transform infrared spectroscopy analysis was prepared by mixing erbium oxide powder with Potassium bromide (KBr) as a host salt, such that 1 part of erbium oxide was mixed with 1000 parts of KBr. The Er_2O_3 and the KBr were then ground in a mortar with the help of a pestle. A little quantity of this powder mixture were then pressed mechanically under a pressure of 5 tons for 10 minutes and a pellet of thickness less than a millimeter obtained.

The host salt is selected on the condition that it will not respond to the infrared spectrum. The region of the spectrum we were interested in was irresponsive for potassium bromide so we found no any contribution from KBr. It occurs sometimes that the KBr absorb some humidity etc from the atmosphere due to its hygroscopic nature and contribute in the sample spectrum. A pellet of the

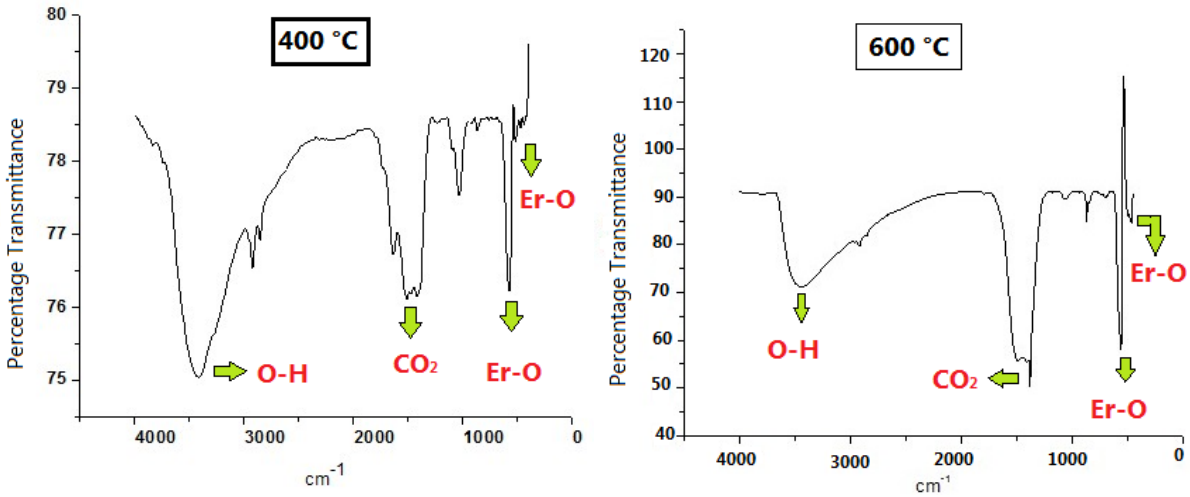

(a) (b)

Figure 4.3: FTIR Spectra of Er_2O_3 (a), sample annealed at 400 ^oC (b), sample annealed at 600 ^oC

potassium bromide was also prepared for taking background spectrum so that it could be neglected. The FTIR spectra was found in agreement with reported spectra for erbium oxide [58]. The FTIR spectra in the range 1200-1400 cm^{-1} is due to the surface activity of the material because of the fact that Er_2O_3 absorb water and carbon di-oxide etc. from the atmosphere. The spectra in the fingerprint region is characteristic of the erbium oxide molecule. The peak at 563 cm^{-1} corresponds to the absorption intensity of Er-O-Er and the peak at 471 cm^{-1} correspond to stretching of Er-O [59]. Comparing both of these spectra it can be concluded easily that as the particle size decreased the surface activity of the particles were found higher due to increased surface area.

4.5 DC Electrical Resistivity

In nano-materials electrical properties depend upon the method of preparation, sintering temperature and grain size. The DC electrical resistivity of the synthesized erbium oxide was measured using two probe method. This method is very fundamental to measure the resistivity of the given sample. It was found that with increase in temperature the resistivity of the erbium oxide decreased. The electrical properties were found associated with semiconductors because the resistivity decrease in semiconductors with rise in temperature as it provides thermal energy to charge carriers so that they can jump from valence to conduction band. The relationship between resistivity and temperature for intrinsic semiconductors can be expressed as

$$\rho = \rho_0 \exp\left(\frac{E_g}{2k_B T}\right) \tag{4.12}$$

where 'k_B' is the Boltzmann constant, 'E_g' is the band gap of the material and 'ρ' is the resistivity

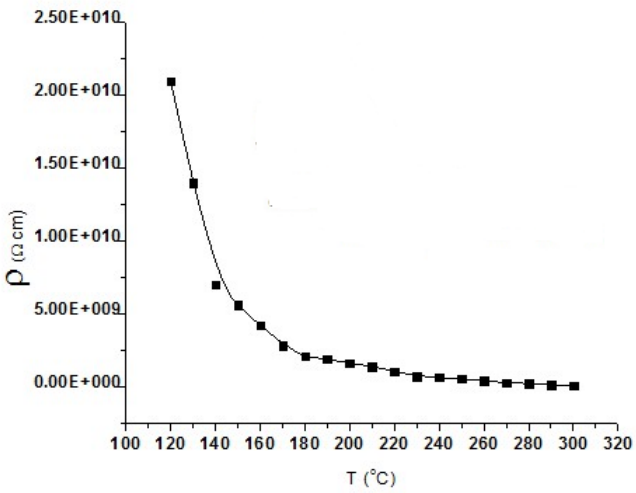

Figure 4.4: Temperature versus Resistivity plot of Erbium Oxide

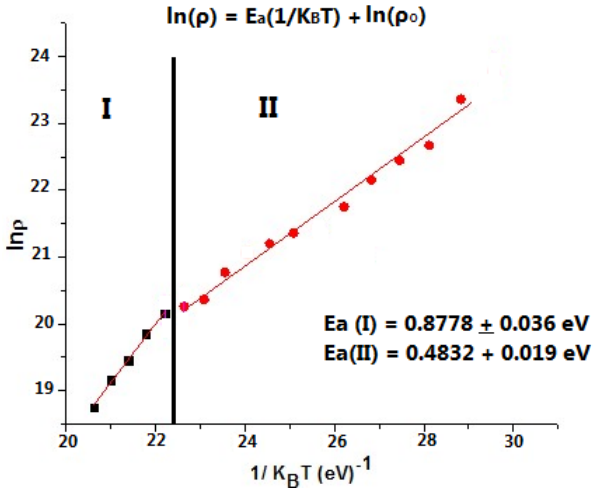

Figure 4.5: Plot of lnρ versus $(1/k_BT)$

of the semiconductor at particular temperature 'T'. The equation can be written as,

$$\rho = \rho_0 \exp\left(\frac{E_{act}}{k_B T}\right), \tag{4.13}$$

where E_{act} is the activation energy of the conduction process. The equation 4.13 is the general equation for semiconductors and semiconductors type materials. Fermi energy level for intrinsic semiconductor lies just in the center of valence and conduction band. But there is no generalized location for the fermi level in the the materials which behave like semiconductor. The plot of lnρ

versus $1/k_BT$ is also shown in fig 4.5. In the electrical behavior of the material a break was noticed around 240 ^oC. This break doesn't corresponds to any transformation of phase [60], because in rare earths oxide the phase transformations occur at very high temperatures. The change of slope in the $\ln\rho$ versus $1/k_BT$, has also been reported for rare earth oxides [61, 63]. Erbium oxide is found to be mixed conductor having major electronic and some ionic contribution for conduction. This break is actually because of the ionic conductivity in the material. At lower temperature the activation energy (E_{act}) of the sample was found smaller (0.483 ± 0.019 eV) while at temperatures above break the activation energy increased to (0.8778 ± 0.036 eV) due to the onset ionic conductivity. As oxygen can diffuse from atmosphere in to these oxides [60], hence give rise to the lattice defects in the material as

$$3/4O_2(g) \quad \leftrightharpoons \quad 1.5O^{2-} \; + \; \square_{Er} \; + \; 3h^+ \tag{4.14}$$

O^{2-} is the oxygen atom at its lattice site, $\square_{Er}$ is cation vacancy and h^+ is a hole. So at the start of conduction the whole contribution was from the electronic conduction and when the temperature increased the ions got some thermal energy and started to move through these created defects as a result of which the activation energy of the material was found to increase.

4.6 Scanning Electron Microscopy of Erbium Oxide

The nanoparticles synthesis is a very delicate process and depends upon many parameters. In the synthesis of nanomaterials the shape of the synthesized particles depends on method of preparation and environmental parameters. If we change the method of preparation or the environmental parameters then the synthesized nanoparticles may have different structure and physical properties. The SEM micrographs of the prepared erbium oxide and energy dispersive spectroscopy was also done on the sample annealed at 600 ^{o}C. To take the SEM micrographs of erbium oxide nanoparticles a suspension of Er_2O_3 was made in ethanol and sonicated for half an hour. A small drop was then spread on a glass substrate which then heated to evaporate ethanol at 50 ^oC in an oven. After that a thin layer of gold particles was coated on the above prepared sample to make it conductive for the machine operation and the similar gold nano particles coating was done on a small piece of pellet. The morphology of pellet is also shown in fig 4.6. The SEM revealed that the nano particles synthesized in the laboratory were spherical in shape with their diameter ranges from 7-38 nm (distribution of particles in this micrograph is shown in the figure 4.6a), while the morphology of pellet is showing agglomerated spherical clusters. The energy dispersive spectroscopy (EDS) imparted that the material prepared were having erbium and oxygen. There is a tiny peak of carbon in the EDS of

pellet in consequence of the surface activity of the material due to its hygroscopic nature. There is no peak of the carbon in the EDS of the nanoparticles because the sample was just prepared at the moment when the SEM micrographs were taken. The exposure of the pellet with the atmosphere was the main reason for the carbon peak.

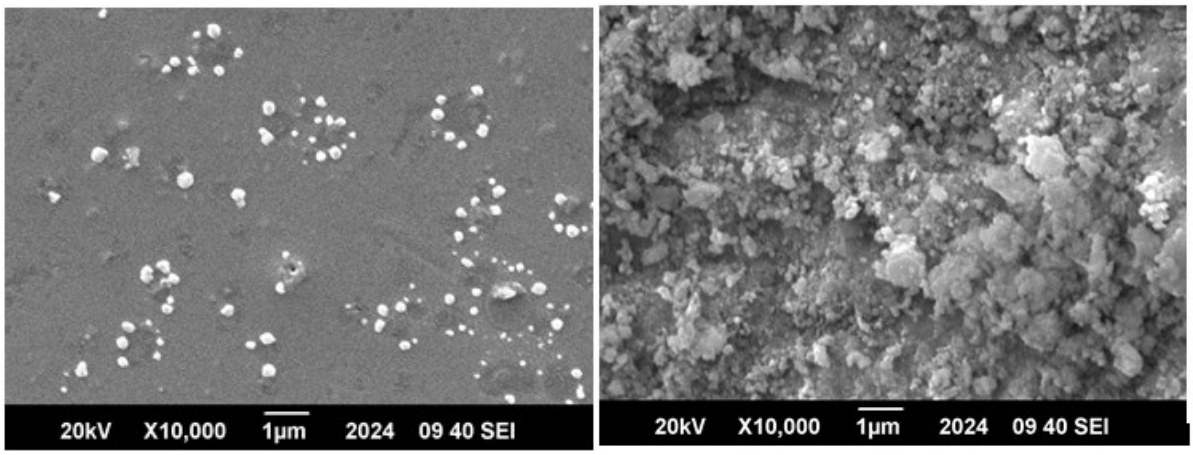

(a) (b)

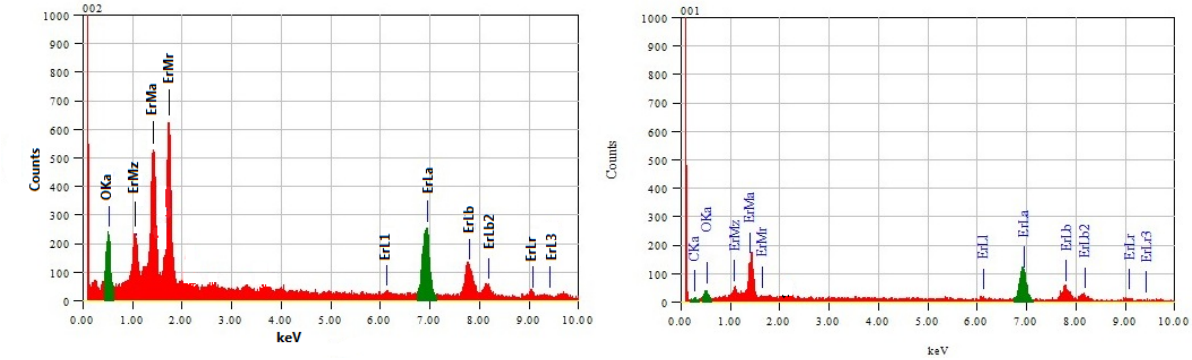

(c) (d)

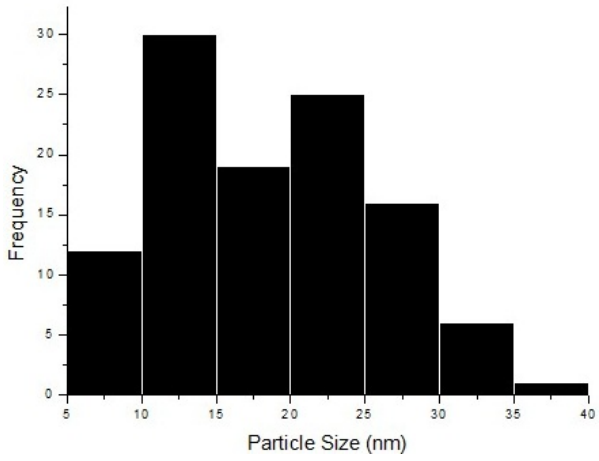

(e)

Figure 4.6: SEM Micrographs and Energy dispersive spectroscopy of Erbium Oxide annealed at 600 ^{o}C: (a) SEM micrograph of erbium oxide nanoparticles, (b) SEM micrograph of the pellet of Erbium oxide, (c) EDS of Erbium Oxide nano-particles, (d) EDS of Erbium Oxide Pellet, (e) Particle size distribution in (a).

4.6.1 Dielectric properties of Erbium Oxide

The dielectric properties of the synthesized particles were studied at room temperature using an LCR impedance analyzer. The properties were studied pellet in the wide frequency range from 100 Hz to 5 MHz.

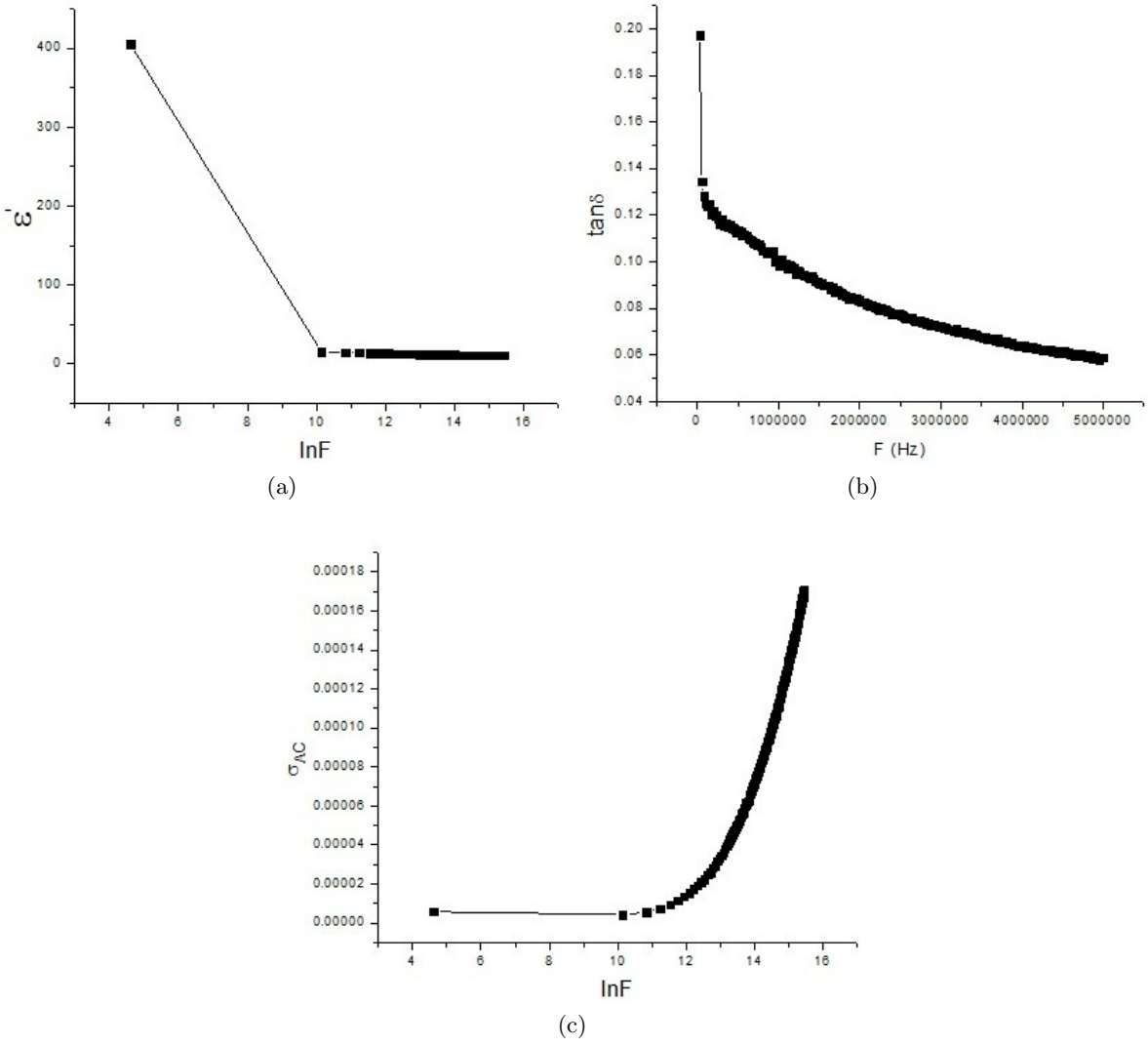

Figure 4.7: (a) Dielectric Constant (ϵ') versus natural log of frequency (lnF) , (b) Loss tangent and frequency plot (F (Hz)), (c) AC conductivity σ_{AC} versus natural log of frequency (lnF) plot

It was found the dielectric constant of the material was having dependance on frequency the increase in frequency caused the dielectric constant of the material to decrease which is due to the decrease in polarization as the frequency increases. This behavior was in agreement with the Maxwell's Wagner Model and Koop's theory of dielectrics. The trend of dielectric loss with the frequency was also noticed and loss tangent was greater for low frequencies but it showed a decreasing

trend on higher frequencies. The high resistivity of the material is the reason for the low dielectric loss. The increase in frequency caused the AC conductivity (σ_{AC}) of the erbium oxide to increase. These dielectric properties were found in agreement with the the trend reported in literature [32] but the erbium oxide nano particles synthesized in this work were having enhanced dielectric properties because of their size and different environmental parameters during their preparation.

4.6.2 Hall Effect Characterization

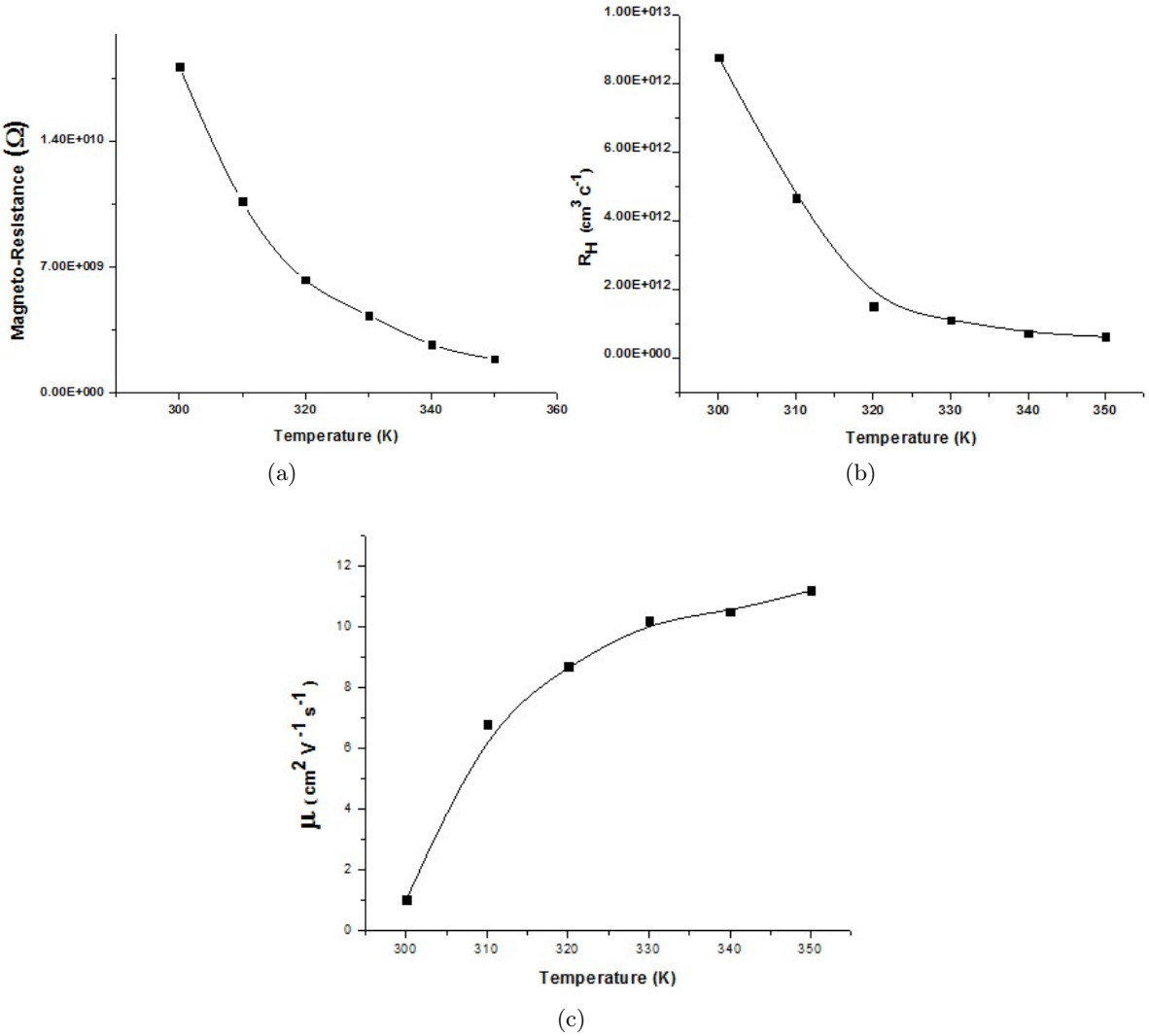

Figure 4.8: Hall characterization of erbium oxide pellet (a) Magnetoresistance versus temperature plot, (b) Hall coefficient (R_H) versus temperature, (c) Hole mobilities versus temperature graph

The Hall effect is a rich source of information for semiconductors and it gives a lot of information about the material in just single characterization. So, Hall effect on the pellet of 997 μm thickness

was studied under a magnetic field strength of 0.55 tesla. The effect of the temperature on the Hall parameters were seen in the range of 300 to 350 K. The magneto resistance (fig 4.8a) showed a decreasing trend in this temperature range which was notice due to increase in carrier concentration (n) as the temperature increased reffadiazad.

The Hall coefficient is an important factor to explain the type of charge carriers in the material [65]. The temperature variation on Hall coefficient was seen (fig 4.8b) and it was found to be positive. So the erbium oxide revealed to be a p-type semiconductor in which majority carriers for conduction are holes. The hole mobility μ_H (fig 4.8c) was also found increasing as the temperature of the sample increased. As temperature increased the carrier mobilities were also found to increase as a consequence its resistivity decreased.

4.7 Erbium Oxide films

4.7.1 Diffraction Pattern of the Erbium oxide films

Erbium oxide layers of thickness in microns were grown on polycrystalline silicon (100) substrate. These film were annealed at 600 ^{o}C so that a crystalline phase in the material could establish. The following fig 4.9 shows the XRD patterns of Erbium oxide layers of thickness in microns. In the

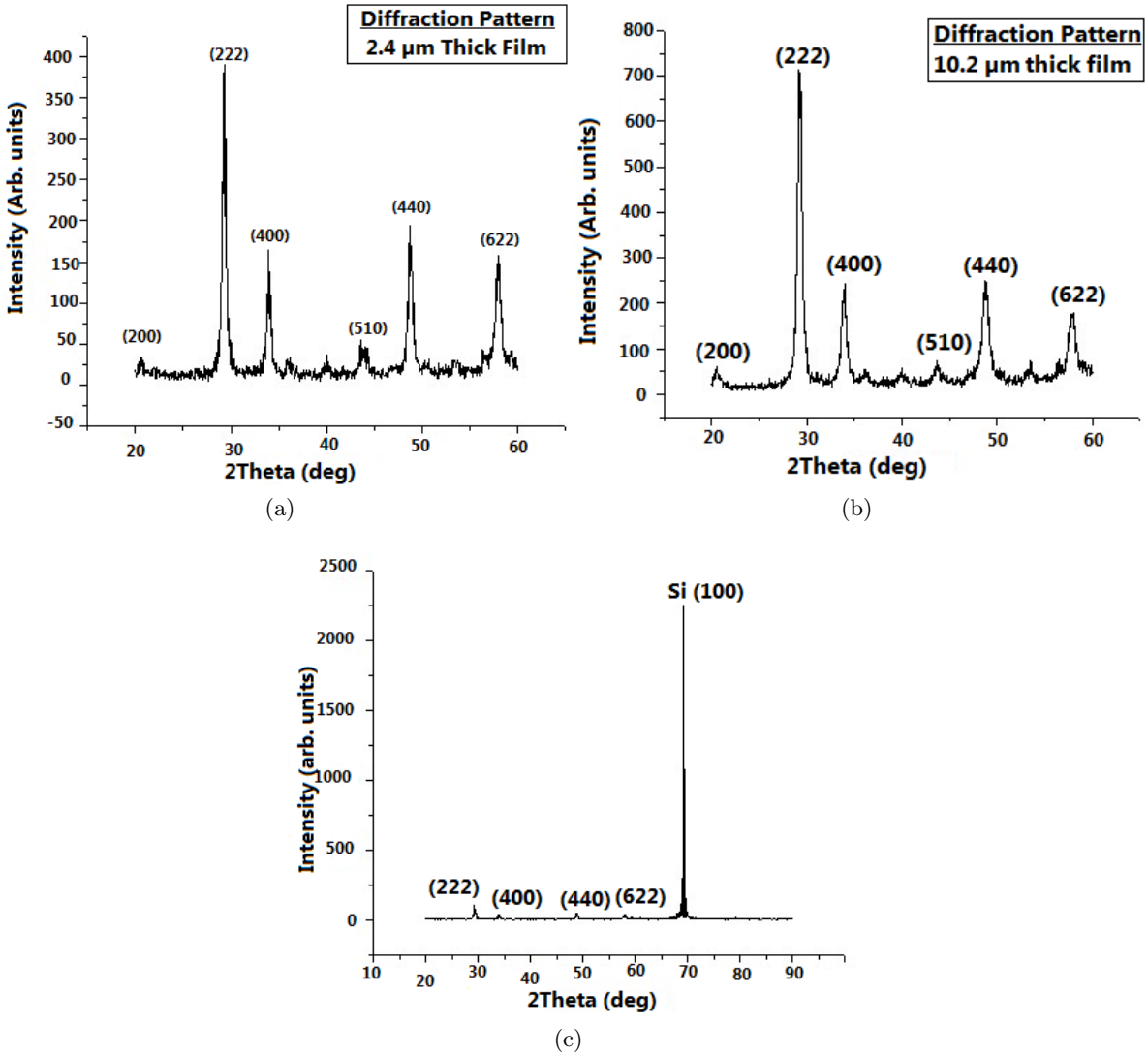

Figure 4.9: XRD patterns (a) Film of thickness 2.4 μm (b), Film of thickness 10.4 μm (c), Substrate Peak along with Erbium Oxide pattern

fig 4.9c the sample was scanned from $2\theta = 20^{0}$ to 90^{o} and the most intense peak was found near $2\theta = 70^{0}$ which is the characteristic peak of substrate Si(100). The peaks of erbium oxide are also indexed in this pattern. Intensity of the peak from the substrate is very high as compared to the

intensity of the peaks from erbium oxide as a result only prominent peak is of Si(100). In order to eliminate this problem the scanning angle (2θ) was kept from ($20\ ^0$ to $60\ ^0$) so that this peak could not dominate. The lattice constant was again found to be 10.558 Å. The average crystallite size in both the samples was calculated using the full width at half maximum of the most intense peak (222) by the Scherrer's formula. It was found to be 20 nm and 25 nm for the layers with thickness 2.4 μm and 10.4 μm respectively.

4.7.2 DC Electrical Resistivity

The DC electrical resistivity of the Erbium oxide films measured in the temperature range 300-350 K. It was found that as the temperature increased the resistivity of the film was decreasing. The activation energy of the films was also calculated and it was noticed to decrease with increase in the thickness of the films. The temperature versus resistivity graph of both the films are shown in fig 4.10 it can also be noticed that the resistivity and thickness of the films are having inverse relationship. While increase in resistivity usually occurs with the increase in activation energy of conductivity. In fig 4.10c the $ln\rho$ versus $(1/K_BT)$ plot is shown. The activation energy was found 0.8426 $\pm$ 0.034 eV for the film of thickness 10.2 μm and 0.9078 $\pm$ 0.089 eV for the film of thickness 2.4 μm. The rise in activation energy decrease the conductivity of the material because a higher amount of energy is required to activate the conduction process.

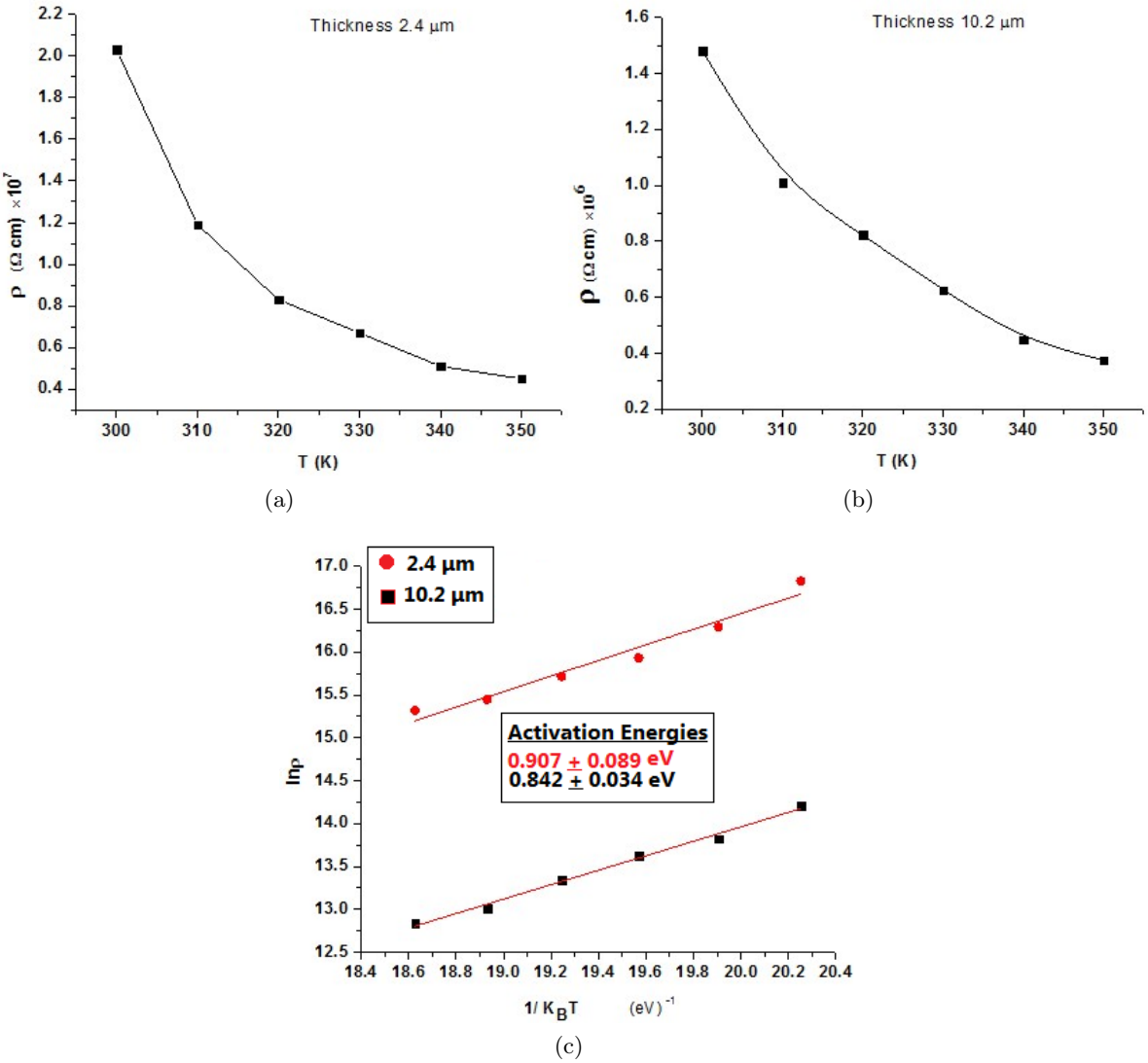

Figure 4.10: (a) Resistivity versus Temperature plot of 2.4 μm thick film (b), Resistivity versus Temperature plot of 10.2 μm thick film (c), ln(ρ) versus ($1/K_B$ T) plot of both films

4.7.3 Hall Effect on films

Hall effect on these synthesized films were studied using HMS (5000) apparatus. Magneto resistance and the Hall coefficient were measured at different temperature of these films and the plot of these parameters is shown in fig 4.11. A decreasing trend with temperature was noticed in both magneto-resistance and Hall Coefficient. The main reason for the decrease in magneto-resistance is the semiconductor behavior of the erbium oxide. While the Hall coefficient were decreasing because of the increase in carrier concentrations at higher temperatures. These measurements also revealed the magneto resistance and Hall coefficient both have an inverse relationship with the thickness of the

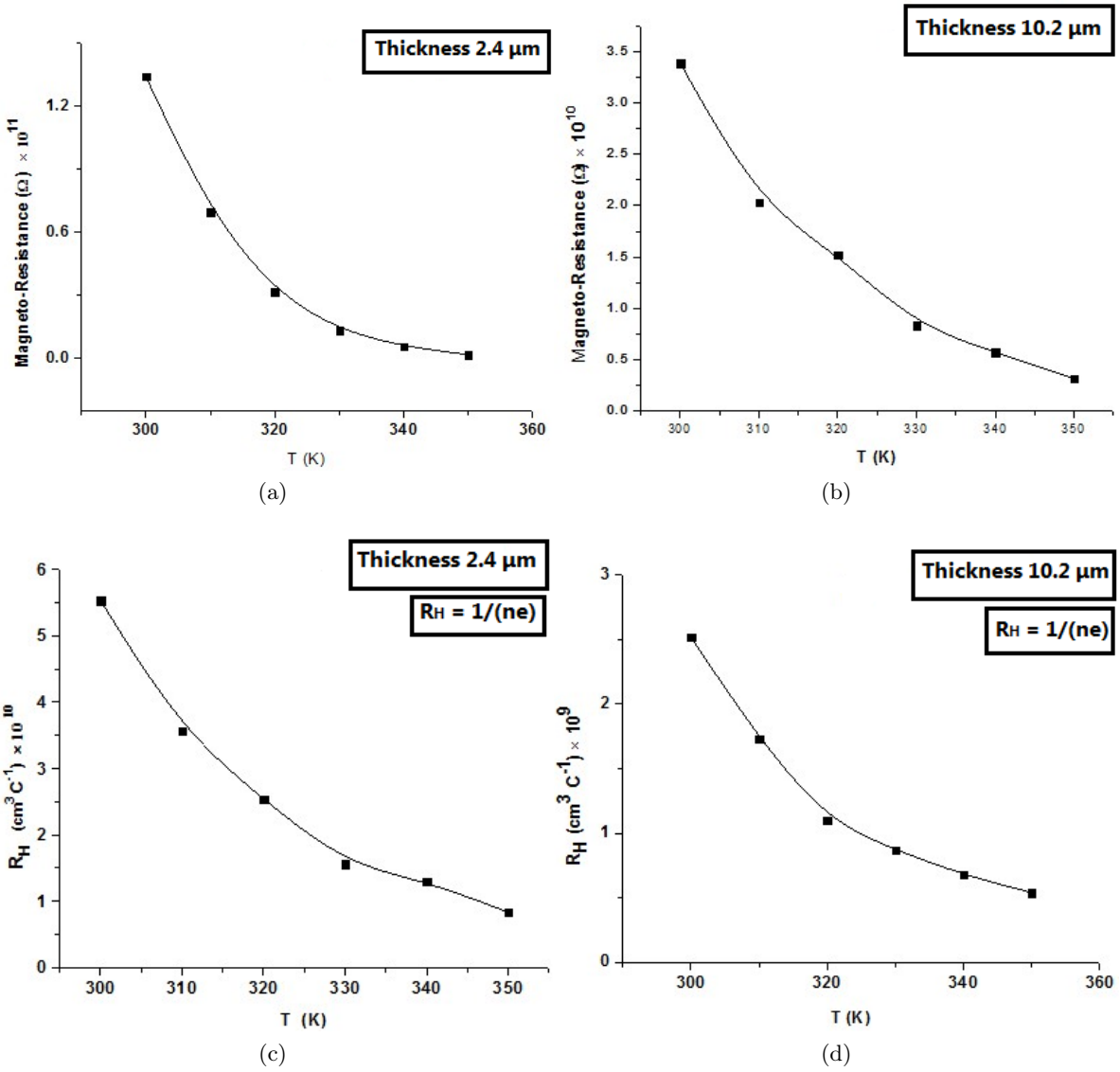

Figure 4.11: (a) Magneto-resistance versus temperature plot of film with thickness 2.4 μm, (b) Magneto-resistance versus temperature plot of film with thickness 10.2 μm, (c) Hall Coefficient versus Temperature plot of film with thickness 2.4 μm, (d) Hall coefficient versus temperature plot of film with thickness 10.2 μm

films.

4.7.4 Scanning Electron Microscopy

The scanning electron microscopy was used to reveal the morphology of the films. The energy dispersive spectroscopy of the samples was also done. The micrographs are showing a flaky morphology in both of the films the figure 4.12a & b are showing these graphs. The energy dispersive spectra of these films are shown in fig 4.12 c & d. EDS results confirmed that the prepared material was

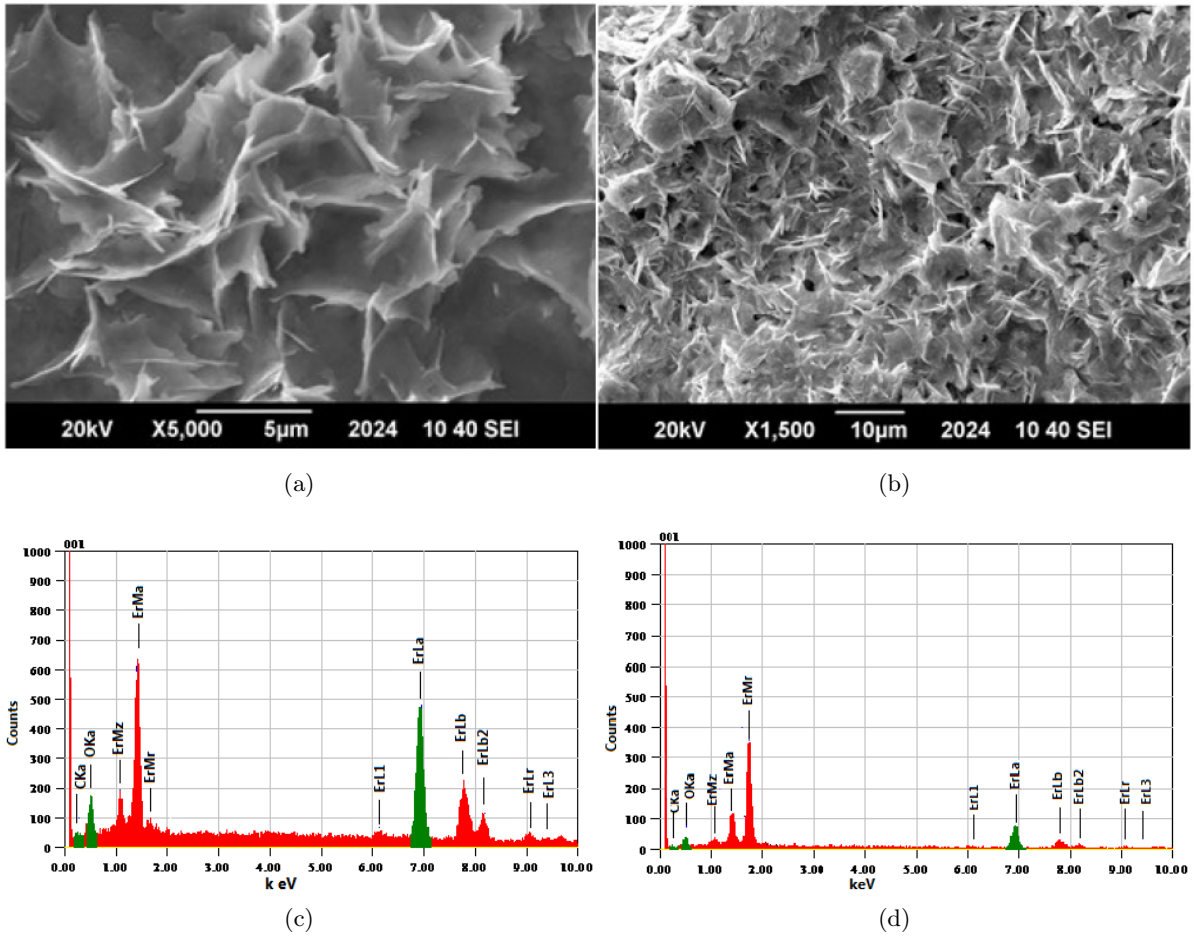

Figure 4.12: SEM Micrographs and Energy dispersive Spectrum : (a) 2.4 μm thick film of erbium oxide , (b) 10.2 μm thick film of erbium oxide, (c) EDS of the sample shown in fig a, (d) EDS of the sample shown in fig b

erbium oxide no other peaks were found rather than a relatively weak peak for carbon. This peak again is coming as a consequence of the surface activity of the erbium oxide. The peak of the carbon in EDS of 2.4 μm film is comparatively more intense than that of the 10.2 μm thick film. The reason is that as the thickness decreases the particle size also decreases as a result of which the surface area increases and so as the surface activity.

Chapter 5

Conclusion and Future Recommendation

The effect of annealing temperature on the crystal structure of laboratory synthesized erbium oxide weas studied in this work using X-ray diffraction (XRD). It was noticed that below 350 ^{o}C the material was completely amorphous, near 400 ^{o}C the crystal structure started to establish and at 600 ^{o}C a completely crystalline phase has been formed and no peak for impurities was found in all the prepared samples. Grain growth was observed as the annealing temperature increased. The XRD density of the prepared sample was in agreement with the density of the pure erbium oxide. Specific surface area was calculated through XRD data analysis and it was found that the surface area has an inverse relationship with particle size.

Furthermore, the specific surface area of the prepared samples were also calculated using and experimental approach. The experimentally measured specific surface area was found in accord with the area calculated using XRD data. This conformance between the two surface areas revealed the reliability of XRD measurements because a decent estimate was made by these results for specific surface area without going in deep experimental measurements. It is suggested that the specific area can be found using the method described in this work for spherical particles.

Fourier transform infrared spectroscopy was carried out on the crystalline samples and it divulged an enhanced surface activity of the erbium oxide particles annealed at lower temperature. Moreover, the FTIR spectra of the erbium oxide showed the characteristic peak of the molecule in the finger-print region. Scanning electron microscopy was used to uncover the morphology of the samples. A spherical morphology was found for particles and an agglomerated clusters of these particles were noticed in the micrographs of pellet. The micrographs for erbium oxide films were having a flaky morphology. Energy dispersive spectroscopy confirmed that the prepared material was completely converted to erbium oxide. The dielectric properties were also found enhanced as compared to the other reported in literature but the trend of the dielectric parameters with frequency was found in

accordance.

Electrical properties have already been studied for rare earth oxides but the electrical properties of erbium oxide are reported for the first in this work. It was noticed that the erbia behaves electrically like semiconductors its resistance decrease with increasing temperature. Erbium oxide was found to be a mixed conductor in which major conductivity is due to p-type electronic contribution and some contribution is from ionic conductivity. The material was found to have a break in the activation energy around 240 ^oC above which activation energy increased because of the ionic contribution in the conductivity. This break in electrical properties was found near to the break that has been reported before for oxide of its neighboring atom Terbium. In order to reveal the type of semiconductor the Hall effect was performed on the pellets and films. Hall characterization suggested the erbium oxide as a potential candidate to find its applications in Hall effect sensors. The sensors based on these materials can work in a wide range of temperature because of the thermal stability at extremely high temperatures and an increased sensitivity of the sensor based on this material at extremely low temperatures.

In the future it would be interesting to work on the following aspects

- The development of the Hall effect sensors based on these materials in the laboratory.
- The use of this material as dopant in other hosts.
- The Hall effect characterization of the other rare earth oxides.
- As these materials have interesting optical and magnetic properties. So the study of these properties would also be a very promising work for the modern technological needs.
- The temperature dependent dielectric properties will also be interesting to know.
- A Hall effect apparatus can be developed in the laboratory for high temperature characterization in the laboratory.

References

[1] "Nanoscience and nanotechnologies:oppourtunities and uncertainities", report by the Royal Society and Royal Acedemy of Engineering (2004)

[2] Luisa Filipponi and Duncan Sutherland, "Introduction to Nanoscience and Nanotechnologies", Aarhus University Denmark (2010)

[3] J L Speshock, R C Murdock, L K Braydich-Stolle, A M Schrand, S M Hussain, J. of Nanobiotechnology **8** (2010) 19

[4] V. Mlinar, Nanotechnology **24** (2013) 042001

[5] J. Shi, Y. Zhu, X. Zhang, Willy R.G. Baeyens, Ana M. Garcaia-Campana, Trends in Analytical Chemistry, **23** (2004) 351

[6] Z. Lu, L. Zhang, L. Wang, Q. Zhang, J. of Nanomaterials, **2012** (2012) 7

[7] S. Besner, M. Meunier, "Laser Precision Microfabrication", Springer (2010)

[8] J. C. Colmenares, R. Luque, J. M. Campelo, F. Colmenares, Z. Karpioski, A. A. Romero, Materials, **2** (2009) 2228

[9] L. Feng, Z. Liu, Nanomedicine **6** (2011) 317

[10] T. J. Simmons, In Nanomaterials for Biomedicine; ACS Symposium Series; American Chemical Society: Washington, DC, (2012)

[11] X. Zhang, Xiaohong Zhang, W. Shi, X. Meng, C. Lee, Shuittong Lee, J. Phys. Chem., **109** (2005) 18777

[12] S. Eustis, M. A. El-Sayed, Chem. Soc. Rev., **35** (2006) 209

[13] Z. Yao, C. Dekker, P. Avouris, "Carbon Nanotubes", Springer (2001)

[14] A. Alagarasi, Introduction to Nanomaterials,(2011) (Unpublished), http://www.nccr.iitm.ac.in/2011.pdf

[15] M. Suzuki, N. Kawamura, H. Miyagawa, J. S. Garitaonandia, Y. Yamamoto, H. Hori, Physical Review Letters, **108** (2012) 047201

[16] X. Teng, Wei-Qiang Han, W. Ku, M. Hucker, Angew. Chem., **120** (2008) 2085

[17] S. Guoa, E. Wanga, Nanotoday, **6** (2011) 240

[18] L. R. Khota, S. Sankarana, J. M. Majaa, R. Ehsania, E. W. Schusterb, Crop Protection, **35** (2012) 64

[19] Z. P. Aguilar, Y. Aguilar, H. Xu, B. Jones, J. Dixon, H. Xu, Y. A. Wang, Nanomaterials in Medicine, **33** (2010) 69

[20] Morris VJ, Trends Biotech., **29** (2011) 509

[21] D. Jariwala, V. K. Sangwan, L. J. Lauhon, T.J. Marksab, M.C. Hersam, Chem. Soc. Rev., **42** (2013) 2824

[22] http://biologicalfuelcell.wordpress.com/biological-fuel-cells/

[23] J.P. Colinge, Chi-W. Lee, A. Afzalian, N. D. Akhavan, R. Yan, I. Ferain, P. Razavi, B. O'Neill, A. Blake, M. White, A-Marie Kelleher, B. McCarthy, R. Murphy, Nature Nanotechnology, **5** (2010) 225

[24] Kjeld Pedersen,"Quantum size effect in nanostructures", Aalborg University.:(2006)

[25] T. Haley,Karl A. Gschneidner,L. Eyring, "Handbook on Physics and Chemistry of rare eath", Elsevier: North Holland (1979)

[26] I. Etchart, Ph.D Thesis: Metal oxides for efficient infrared to vissible upconversion, University of Cambridge, (2010)

[27] G. Moore, Electronics, **38** (1965) 4

[28] J.Robertson, The Europian Physicsl Journal of Applied Physics, **28** (2004) 265

[29] M.P.A. Neuman, R. Romero, K.J. McClellen,J.J. Petrovic, "Fabrication and properties of erbium oxide," Wiley, (1997)

[30] C.H.C. Kao, H. Pan, Y. T. Chiu, J.S. Lu, T. Chang, Solid State Communications, **152** (2012) 504

[31] A. Bakhsh, MS Thesis:Dielectric characterization of rare earth based ceramics,high-k materials:future of microelectronics, SCME NUST (2012)

[32] A. Bakhsh, A. Maqsood, Electronic material letters, **8** (2012)605

[33] M.P. Singh, C.S. Thakur, K. Shalini, N. Bhat, S.A. Shivashakar, Appl. Phys. Letters, **83** (2003) 2889

[34] V. Mikhelashvili, G. Eisenstein, Appl.Phys.Letters **80** (2002) 2156

[35] M. Miritello, R. Lo Savio, A. M. Piro, G. Franzo, F. Priolo, F. Iacona, C. Bongiorno, Journal of Applied Physics, **100** (2006) 013502

[36] D. Levchuk, S. Levchuk, H. Maier, H. Bolt, A. Suzuki, J. of Nucl. Mater., **367** (2007) 1033

[37] https://www.llnl.gov/str/May05/Satcher.html

[38] Charles Kittel, "Introduction to Solid State Physics", John Wiley and Sons Inc.:Newyork (1976)

[39] http://en.wikipedia.org/wiki/Scanning_electron_microscope

[40] G. Z. Cao, Y. Wang, "Nanostructures and Nanomaterials: Synthesis, Properties and Applications", World Scientific Publishing Co. Pte. Ltd.

[41] http://www.purdue.edu/rem/rs/sem.htm

[42] http://chemistry.oregonstate.edu/courses/ch361-464/ch362/irinstrs.htm

[43] S. Brunauer, P. H. Emmett, E. Teller, J. Am. Chem. Soc., **60** (1938) 309

[44] A. J. Ihde,"The development of Modern Chemistry", Courier Dover Publications (1984)

[45] K. M. Hubbard, B. F. Espinozo, Thin Solid Films, **366** (2000) 175

[46] B. A. Pint, P. F. Tortorelli, A. Jankowski, J. Hayes, T. Muroga, A. Suzuki, O. I. Yeliseyeva, V. M. Chernov, J. Nucl. Mater., **119** (2004) 329

[47] A. Sawada, A. Suzuki, H. Maier, F. Koch, T. Terai, T. Muroga, Fusion Eng. Des., **737** (2005) 75

[48] F. Koch, R. Brill, H. Maier, D. Levchuk, A. Suzuki, T. Muroga, H. Bold, J. Nucl. Mater. **1403** (2004) 329

[49] D. Levchuk, S. Levchuk, H. Maier, H. Bolt, A. Suzuki, J. Nucl. Mater., **1033** (2007) 367

[50] X. Chen, C. Wang, X. R. Hu, K. Stahl, J. Jiang, Nanotechnology, **22** (2011) 295708

[51] R. Scheps, Progress in quantum electronics **20** (1996) 271

[52] L. David,"Handbook of Chemistry and Physics", CRC press (1998)

[53] M. Miritello, R. Lo Savio, A. M. Piro, G. Franzo,F. Priolo, J. Appl. Phys., **100** (2006) 013502

[54] S. H. Hosseini,S. H. Mohseni, A. Asadnia, H. Kerdari, Journal of Alloys and Compounds (2010)

[55] M. Lequitte, D. Autissier, Nanostructured Materials, **6** (1995) 333

[56] W.M Keely, Anal. Chem., **38** (1966) 147

[57] M.George,S. S. Nair,A.M. John,P.A. Joy, M.R. Anatharman, J. Phys. D: Applied Physics, **39** (2006)900

[58] X. Dong,G. Hong, J. Mater. Sci. Technol, **21** (2005) 555

[59] Shruti Badhwar, "Nanoelectronics: Device Fabrication and Characterization", (Unpublished) (www.jncasr.ac.in/shruti/labreport5.pdf)

[60] G. V. Subba Rao, S. Ramdas, P. N. Mehrotra, C. N. R. Rao, J. Solid state Chem., **2** (1970) 377

[61] P. N. Mehrotra, G. V. Chandrshekar, E. C. Subbarao, C. N. R. RAO, Trans. Faraday Sot., **62** (1966) 3586

[62] P. N. Mehrotra, Ph.D. Thesis, Indian Institute of Technology Kanpur, 1967

[63] G. Brauer, R. Muller, Z. Anorg. Allgem. Chem., **321** (1963) 234

[64] Fahad Azad, A. Maqsood, Electronic Materials Letters, (In press)

[65] K. Singha, V. K. Singh, B. C. Yadav, Int. J. of Chem. and Anal. Sci., **2** (2011) 136